12-4-2006

DNA Photocleavage by Acridine and Phenazine-Based Chromophores

Earl John Fields

Follow this and additional works at: http://scholarworks.gsu.edu/chemistry_theses

DNA Photocleavage by Acridine and Phenazine-Based Chromophores

by

Earl J. Fields, Jr.
Under the Direction of Dr. Kathryn B. Grant

ABSTRACT

Photodynamic therapy (PDT) is a promising approach used in the treatment of cancer, age related macular degeneration, psoriasis, and other diseases. Our research is focused on the discovery of new photonucleases for use in PDT. This study evaluates the photo-induced DNA cleaving abilities of a series of acridine and phenazine-based chromophores. The extended, aromatic ring systems of these compounds are expected to intercalate between adjoining base pairs in the DNA double-helix. Once irradiated, strand breakage, or nicking of plasmid DNA is achieved at micromolar concentrations of compound (pH 7.0 and 22 °C). Our scavenger experiments show that this process occurs as a result of direct electron transfer to oxygen and/or by means of energy transfer which results in the production of singlet oxygen. Three of the photonucleases being examined were designed to chelate metal. These exhibited increased levels of DNA photocleavage in the presence of copper(II).

INDEX WORDS: Photodynamic therapy, Intercalator, Photocleavage, Acridine, Phenazine, Thesis, Graduate office, Earl Fields, Jr., Master's degree, Georgia State University

DNA PHOTOCLEAVAGE BY ACRIDINE AND PHENAZINE-BASED

CHROMOPHORES

by

EARL J. FIELDS, JR.

A Thesis Presented in Partial Fulfillment of Requirements for the Degree of
Master of Science

in the College of Arts and Science

Georgia State University

2006

DNA PHOTOCLEAVAGE BY ACRIDINE AND PHENAZINE-BASED

CHROMOPHORES

by

Earl J. Fields, Jr.

Committee: Dr. Kathryn B. Grant
                         Dr. Dabney W. Dixon
                         Dr. Alfons L. Baumstark

Electronic Version Approved:

Office of Graduate Studies
College of Arts and Sciences
Georgia State University
December 2006

Table of Contents

List of Tables

List of Figures

List of Abbreviations

$A_{highest}$ Highest recorded absorbance in a given series of measurements

A_{lowest} Lowest recorded absorbance in a given series of measurements

bp   base pair

CT-DNA   calf thymus DNA

DMSO   dimethyl sulfoxide

dsDNA   double-stranded DNA

DSB   double-stranded break

eV   electron volts

H_2O_2 hydrogen peroxide

MeV   mega electron volts

NaCl   sodium chloride

NaN_3 sodium azide

$^1O_2$ singlet excited state oxygen

$^3O_2$ triplet ground state oxygen

$O_2^{\bullet-}$ superoxide anion radical

$^{\bullet}OH$ hydroxyl radical

PDT   photodynamic therapy

SC   supercoiled

SOB   super optimal broth

SOD   superoxide dismutase

ssDNA   single-stranded DNA

T_m melting temperature

TAE   tris-acetate-EDTA

Tris   tris(hydroxylmethyl)aminomethane

UV-vis   ultraviolet-visible

Introduction

Photodynamic therapy (PDT) is a promising approach used in the treatment of cancer, age related macular degeneration, psoriasis, and other diseases. In PDT, a light source is utilized to activate a photosensitizing agent which selectively destroys diseased tissue. The patient is administered the photosensitizing compound hours or days before the procedure. The compound will be absorbed by cells throughout the body, but it may be preferentially retained by tumor cells. It is therefore essential that the compound be nontoxic until activated by light. During the procedure, the diseased tissue is irradiated at a specific wavelength where the compound absorbs. The compound then causes damage to the DNA and other cellular components in the irradiated area, leaving other healthy cells intact.

The use of light as a therapeutic agent is not a new concept. Light has in fact been used for more than three thousand years as a form of medicinal therapy. [1,2] There is evidence that ancient Egyptian, Chinese and Indian civilizations used light to treat various diseases including psoriasis, vitiligo, and even skin cancer.[3] Documents have been found from the 2nd century B.C. in which Greeks described the use of "heliotherapy" as an efficient means of the "restoration of health". In the Hindu sacred text *Atharva-veda*, which dates back to 1400 B.C., there is reference to the usage in India of seeds from the plant *Psoralea corylifolia* and sunlight as a treatment for vitiligo. Similar references were found in Egyptian writing regarding the use of the plant *Ammi majus*, which was also used to treat vitiligo.

In 1815, J. F. Calvin wrote about what he referred to as the curing effect that sunlight appeared to have on various conditions such as rickets, scrofula, scurvy,

rheumatism, paralysis, and muscle weakness.[1] It was not until 1822 when a Polish physician, Dr. Sniadecki formally documented the importance of exposure to the sun as a means to prevent and cure rickets. The current usage of light in targeted medical therapy has its most direct origins at the turn of the nineteenth century.[1]

In 1900, a German medical student named Oscar Raab found that certain wavelengths of light were lethal to microorganisms, such as *Paramecium*, when irradiated in the presence of acridine.[4] Also in that same year, the French neurologist J. Prime noted that epilepsy patients, who were receiving the oral medication Eosin, developed severe cases of dermatitis in the areas of their body which had been exposed to sunlight.[5] In 1903, Herman von Tappeiner, director of the Pharmacological Institute of the Ludwig-Maximilians University in Munich, and A. Jesionek topically applied eosin to von Tappeiner's skin and irradiated the area with white light.[6] Tappeiner noted a sensitivity and reddening of the skin in the areas exposed to light where the Eosin had been applied. They document this phenomenon and named the process photodynamic action, the first known usage of the term.[7] von Tappeiner is considered to be one of the pioneers in the field of photobiology.

During the same period (the late 1890s), a scientist working in Denmark, Niels Finsen, was developing a similar process using light to treat disease. In 1901, he discovered that exposing smallpox pustules to red light would prevent the formation and discharge of the pustules.[8] He also discovered that solar ultraviolet light could be used to cure cutaneous tuberculosis. For his efforts, Finsen was awarded the 1903 Nobel Prize in medicine. He is also credited with the origin of modern light therapy.

Some of the first compounds found to be effective in phototherapy were porphyrins, which continue to be the most widely studied class of photosensitizers. Among the first documented studies with these compounds is the work conducted by W. Hausmann around 1911. He used a haematoporphyrin, which he isolated from blood samples, and found that upon irradiation with light, red blood cells as well as skin cells and paramecia were destroyed.[9]

The first documented photodynamic therapy studies involving humans are from the laboratory of Friedrich Meyer-Betz, a German scientist who in 1913 injected himself with a 200 mg sample of haematoporphyrin. He observed that in those areas exposed to light, after the haematoporphyrin had been intravenously administered, there was significant discomfort and swelling.[10] A report published in 1943 documenting the work of Auler and Banzer presented the first successful usage of the photosensitizer haematoporphyrin and light to treat a localized tumor.[11] At that time, there was also a growing belief that the compound haematoporphyrin was preferentially taken up by tumor cells. This conclusion was based largely on the observation by Auler and Banzer that, upon injection with haematoporphyrin IX, the compound accumulated in primary and metastatic tumor cells as well as in lymph nodes. They then found that subsequent treatment of the tumors with light showed very positive results: those mice with tumors tolerated a larger dose of the compound. They concluded that this was probably because tumor cells took up significant amounts of the compound, thus protecting other sensitive organs from the effects of the radiation damage. [11]

In the 1950s, the use of phototherapy became widespread. The English obstetrician Richard Cremer, on the recommendation of a local nurse in Essex, England, began using phototherapy as a treatment for jaundice in newborns babies.[12]

The idea of haematoporphyrin uptake in humans prevailed until the mid-1950s when the Israeli researcher S. Schwartz proposed that this phenomenon might not be due to haematoporphyrin itself, but rather due to some impurity present in the mixture being employed. This was attributed to the fact that the mixture had never been completely characterized and remained quite difficult to purify. In his work, Schwartz had injected over 150 mice with varying amounts of haematoporphyrin from 10 μg up to 1250 μg. After an incubation time of three hours, the mice were exposed to ionizing radiation. Those mice receiving intermediate doses of the compound, around 50 μg, showed complete destruction of the tumor, while those receiving very high or very low doses did not show complete destruction. Schwartz went through great efforts to purify the commercial samples of haematoporphyrin and found that the pure haematoporphyrin was a very poor photosensitizer. He then treated the purified haematoporphyrin with acetic acid which yielded a product that was a more effective photosensitizer.[13] Further research by R. Lipson *et al*. working at the Mayo Clinic showed that chemically modifying the structure of haematoporphyrin could increase the selective uptake of the compound by cancer cells.[14] They named the resulting compound haematoporphyrin derivative (HpD). This became the first synthetic compound to be employed in the localized photo treatment of tumors. Work on this compound continued through the sixties and into the early seventies, showing that the selective uptake of HpD could be greatly increased if the compound were administered intravenously or intraabdominally,

and could serve as a very effective tool for the detection of cancers. Also, prolonged irradiation of tumor cells sensitized with HpD was found to effectively destroy these cells. Lipson and his colleagues were able to determine that the HpD derivative they had synthesized was actually an aggregate containing many different components, primarily composed of several different porphyrin monomers, as well as dimers and several oligomers. They discovered that each of these three groups of compounds had very different properties and reacted differently in cell culture and had very different degrees of efficacy as photosensitizes. The monomers were found to have high fluorescence quantum yields but exhibited very poor cellular uptake. The dimers had better cellular uptake capacity, but exhibited relatively low fluorescence quantum yields. The aggregates were shown to have very weak fluorescence quantum yields, but were taken up most effectively by tumor cells.[14] Then, in 1975, Thomas Doughtery and his associates working at the Roswell Park Memorial Cancer Institute in Buffalo, N.Y., further purified HpD by removing the monomers and produced the first FDA-approved phototherapeutic agent, Photofrin I.[15] They reported that this compound in combination with irradiation using red-light stopped mammary tumor growth. It was used for the treatment of skin, brain and bladder tumors in humans.[16, 17] It was also employed for the temporary relief of other conditions including endobronchial and esophagus obstructions.[18] In 1975, J.F. Kelly reported that the compound proved to be effective in the treatment of bladder carcinoma in mice.[19] Then, in 1976, Kelly and associates initiated the first human trials with HpD for the diagnosis of cancer. After observing that there was significant accumulation of HpD in malignant and premalignant bladder tissue but not in healthy tissue, Kelly hypothesized that by attaching a fluorescent chromophore

to the HpD molecule, it could be possible to screen patients for the presence of malignant tissue.[20] These discoveries were pioneering in the field of photodynamic therapy as a means of detecting and eradicating malignancies.

Once it was realized that haematoporphyrin and HpD were both mixtures with components containing very different properties, there was a great deal of interest in developing a pure photosensitizing agent. In 1972, I. Diamond and his colleagues theorized that by combining the best tumor-localizing and tumor-phototoxic properties of porphyrins, it might be possible to design an efficient cancer killing agent.[21] Because of its low extinction coefficient and varying levels of purity, Photofrin I required large doses. In addition, it was difficult to calibrate usage for individual patients. Also, because of the slow cellular uptake and clearance rates, the compound needed to be administered two to three days prior to treatment and had lasting side effects which could persist up to six weeks following treatment. Irradiation at the wavelength maximum of this compound, 630 nm, provides poor tissue penetration by the light. Its applications are limited to treatment of near surface carcinomas. Effective penetration into tissue is seen at wavelengths of 600-800 nm,[22-26] with increasing tissue penetration being in direct correlation to increasing wavelength. In 1983, these shortcomings led to the development of a more effective version of Photofrin by Kessel and Crow referred to as Photofrin II. Today, Photofrin II is the only drug approved by the U.S. FDA for the treatment of superficial bladder carcinoma; it is also being used in Canada for similar treatments and is approved for use in early lung and esophageal cancers in both Japan and the Netherlands.[27] As of March 2006, there were three approved compounds and several compounds in clinical trials awaiting approval by the U.S. FDA (Table 1).

Sensitizer	Trade Name	Applicaion / Condition	FDA Status
HpD porfimer	Photofrin II	Cervical, endobronchichial bladder, gastric cancers and brain tumors	Approved
BPD-MA benzoporphyrin derivative monoacid	Verteporfin/ Visudyne	Macular degeneration	Approved
5-ALA 5-aminolevulinate	Levulan	Actinic keratosis	Approved
hexaminolevulinate hydrochloride	Hexvix	Diagnosis, bladder cancer	PHASE III
SnET2 tin ethyl etiopurpurin	Photrex	Wet macular degeneration	PHASE III
Anecortave acetate	Retaane	Wet macular degeneration	PHASE III
8-methoxypsoralen	Methoxalen	T-Cell lymphoma, psorasis	PHASE III
Dihematoporphyrin derivative	Prednisolone	Macular degeneration	PHASE III
5-ALA methyl aminolevulinate	Metvix	Pre-cancerous lesions, actinic keratosis, basal cell carcinoma	PHASE II
5-ALA benzylester 5-aminolevulinate benzylester	Benzix	Intestinal cancer	PHASE II
Taporfin	Talaporfin	Solid tumors	PHASE II
Diethylene glycol benzoporphyrin	Lemuteporfin	Prostate hyperplasia	PHASE II
Lutetium texaphyrin	Motexafin Lutetium	Stage I & II prostate cancer / recurrent prostate cancer	Completed PHASE I
M-THPC *meta*-tetrahydroxyphenylchlorin	Foscan	Prostate and pancreatic tumor	PHASE I
HPPH 3-(4- hydroxyphenylpropionic acid hydrazide HCl	Photochlor	Basal-cell carcinoma	PHASE I
Phthalocyanine-4	Pc 4	Cutaneous/subcutaneous lesions	PHASE I
Silicone phthalocyanine-4	Si Pc4	Actinic keratosis	PHASE I
Lutetium texaphyrin	Lutex	Cervical, prostate and brain tumors	Suspended
Boronated protoporphyrin	BOPP	Brain tumor	Withdrawn (Phase I)

Table 1 PDT agents and their status as of March 2006.

metalloporphyrin

metallochlorin

metallonaphtalocyanine

metallophthalocyanine
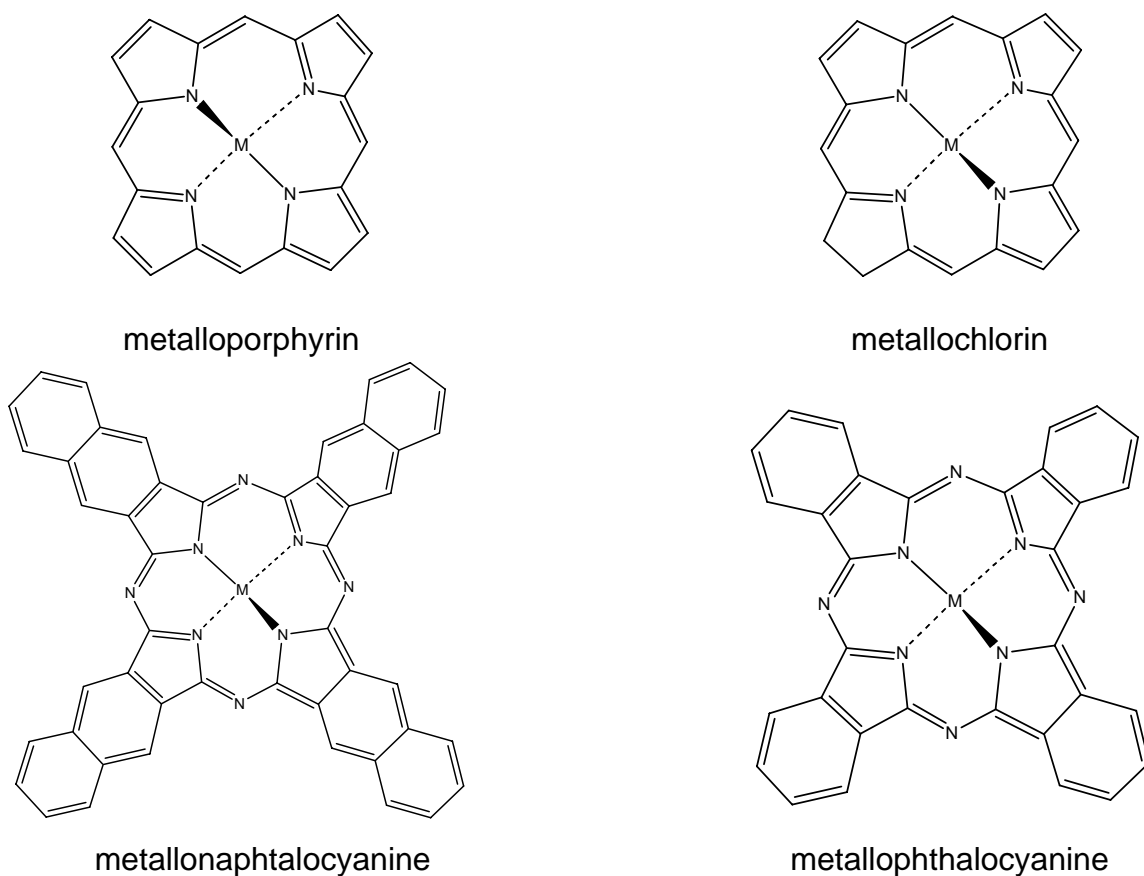
Figure 1 Porphyrin-derivatives and their structures.

Compounds in these classes, and other similar ones, currently under investigation as potential photosensitizers are referred to as "second generation" and "third generation" photosensitizers. They include other porphyrin derivatives such as phthalocyanines, napthalocyanines, and chlorines (Figure 1). A number of the compounds listed in Table 1 are those in which aminolevulinate derivates are enzymatically converted *in vivo* to protoporphyrin IX. This compound is a precursor to the production of other porphyrins. In 1961, Wilkman introduced tetraphenyl porphyrin sulfonate (TPPS) and proposed it as a good alternative to HpD. It was suggested that it would have a much better ability to localize in tumor cells. Pthalocyanines were first introduced by Ben-Hur *et al.* in a 1985 journal article which described the ability of this class of compounds to inhibit tumor

growth in Chinese hamsters.[28] Both these compounds can be synthesized with variable numbers of sulfonate groups, which allow for specific tuning of the compounds, making them more or less water-soluble as desired. This ability has led researchers to investigate how different properties and the structure of the compound will affect function. Chlorin compounds were first introduced into the area of photodynamic therapy in 1986 by Berenbaum and colleagues with a *meso* chlorin-substituted tetra (*meta*-hydroxyphenyl) chlorin. This compound was suggested to have a favorable selectivity for tumor cells.

A major advantage in the development of these compounds is that they are well characterized. Most are very efficient generators of singlet oxygen and have high fluorescence quantum yields which correlate to high λ_{max} absorbance. In addition, any new compounds should have a consistent composition inactive until irradiated and be chemically stable. These compounds should also exhibit a high selectivity for malignant tissues and relatively rapid elimination from healthy tissue. These factors would help alleviate some of the common problems currently experienced by patients undergoing photodynamic therapy with Photofrin I and II. A major challenge, however, is that many are hydrophobic, which can cause the compounds to aggregate or stack in aqueous environments. As a result, equally important in the development of new drugs is an effective delivery system. There are numerous, proposed systems including polymeric particles, oil-dispersions, hydrophilic polymer-photosensitizer conjugates, and liposomes.[29-32]

In PDT, electromagnetic radiation emitted by a light source is absorbed by a phototsensitizer giving the singlet state ($^1P^*$, Figure 2). The singlet state can undergo intersystem crossing to a long-lived triplet state ($^3P^*$). The generation of cytotoxic species

can occur from either the single state or the triplet state through two possible pathways, know as Type I and II processes (Figure 3).[33] However, because of the significantly
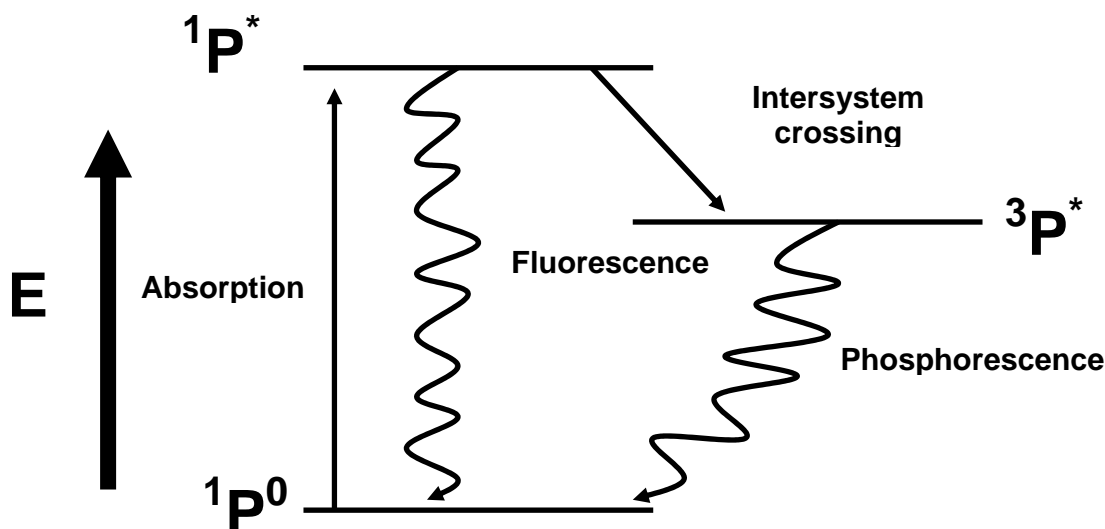
Figure 2 Jablonski Diagram**.** Once the photosensitizer is irradiated by an appropriate light source, it can absorb the energy to give an excited state. The photosensitizer can then react chemically, release the energy through fluorescence, or it may undergo intersystem crossing to a lower energy, longer lifetime triplet excited state. This energy can decay further back to the ground state through phosphorescence. Alternatively, the triplet state may transfer this energy to a nearby species capable of accepting the energy such as molecular oxygen which exits in a triplet ground state.

longer lifetimes, (τ_T), observed for the triplet state, compared to the 10-100 ns lifetimes typically seen for the singlet state,[34] cytotoxic species are most often produced from the triplet state. Because the triplet state is a low energy state, it has the advantage of having a significantly longer lifetime, usually greater than 500 ns.[35]

The DNA strand breaks induced by photosensitization can occur as a result of three primary mechanisms: 1) photo generation of hydroxyl radicals (•OH; Type I pathway), a reactive oxygen species that cleaves DNA by abstracting hydrogen atoms from the deoxyribose sugar backbone, 2) electron transfer from the nucleobases, specifically guanine, to the photochemically excited state of the photosensitizer (Type I

pathway), 3) preferential oxidation of guanine by singlet molecular oxygen ($^1O_2$) generated via energy transfer from the excited photosenstizer (Type II pathway).[35-38]
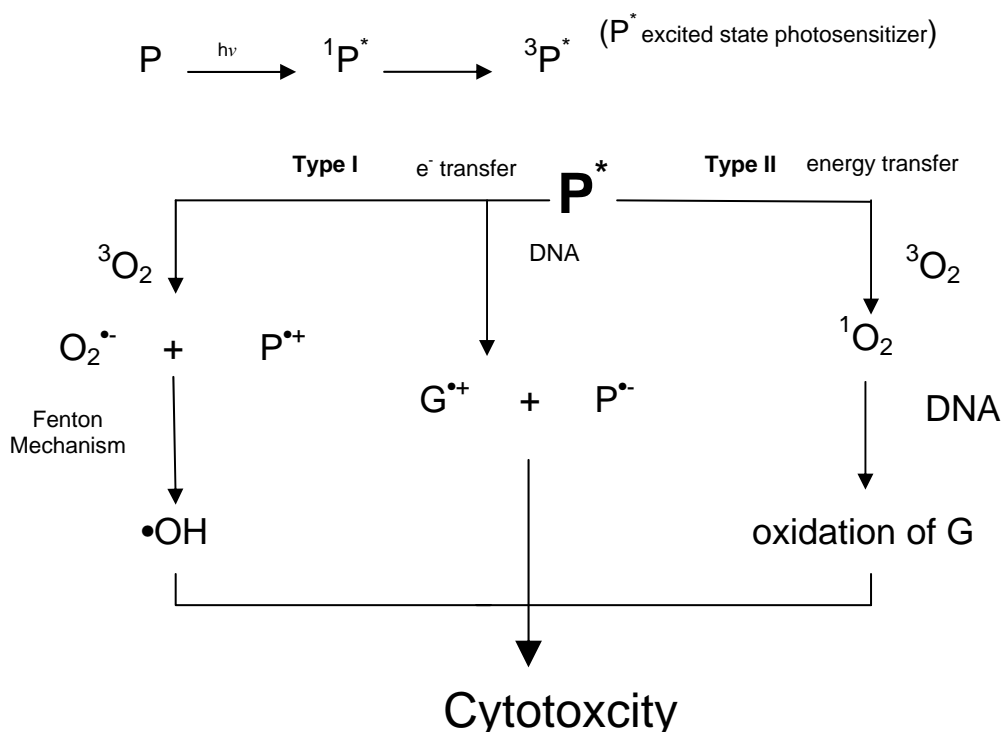
Figure 3 Photocleavage by Type I & II Pathways. Once entered into an excited state, the sensitizer may transfer its energy to the ground triplet state of oxygen exciting oxygen to a singlet state via the Type II pathway. Alternatively, the photosensitizer may be oxidized through the loss of an electron to a nearby species capable of accepting an electron such as a oxygen molecule. This electron transfer may then induce deoxyribose hydrogen atom abstraction, via the production of cytotoxic hydroxyl radicals (·OH). The excited photosensitizer may also be reduced by accepting an electron from DNA. Although the Type I plays a relatively minor role in PDT compared to Type II, both can serve to damage DNA and other biomolecules which may subsequently induce necrosis and/or apoptosis of living cells.

The triplet lifetime is defined as the average time a molecule spends in an excited triplet state. Having a long triplet lifetime is therefore a key factor in the development of new photosensitizers. The triplet state energy of the photosensitizer can then easily be transferred to another molecule which is located in close proximity. Oxygen ($^3O_2$) is one of the few molecules which possess a triplet ground state. The energy of the oxygen excited singlet state is 7900 cm^{-1}. Therefore, molecules which have triplet states with

lower energy will be unable to excite molecular oxygen from its ground triplet state to the higher excited singlet state. It has also been noted that molecules with much greater energies, above 18,000 cm^{-1}, can lead to unfavorable Franck-Condon factors, which may inhibit the transfer of energy between these two species. Molecules with triplet state energies between 7900 and 18000 cm^{-1} are therefore needed to initiate a Type II photosensitization reaction for use in PDT. [34-37] Singlet oxygen is a strong electrophile, which can induce significant damage to surrounding tissue, diffusing as far as 100 nm during its lifetime. [38]

Those molecules which do not possess sufficient energy to excite the molecular oxygen ground state may still be candidates for use in PDT by means of the alternative Type I pathway (Figure 3). This pathway involves a process in which direct transfer of electrons from DNA nucleobases to the photosensitized triplet occurs. The photosensitized triplet can also transfer electrons to ground state oxygen, $^3O_2$, to form superoxide anion radicals ($O_2^{\cdot-}$). The superoxide anion radical production can lead to the formation of hydroxyl radicals by a Fenton mechanism. As mentioned previously, hydroxyl radicals then cleave the DNA phosphodiester backbone by a mechanism that involves abstraction of hydrogen atoms from deoxyribose.[39] Both singlet oxygen and hydroxyl radicals can damage cellular components, including DNA, proteins and other macromolecules. This leads to the destruction of cells through apoptosis and/or necrosis.

There is an indication that there may be additional therapeutic benefits arising from PDT. Inaba *et al.* have shown that apoptotic cells often serve as triggers leading to various immune responses. This is because they often produce antigens which are recognized by the immune system. It is often the case, however, that cancer cells are not

sufficiently immunogenic to trigger this response *in vivo*.[40, 41] This is due in part to the fact that most tumor antigens are masked or made inaccessible by cancerous growths. It has been shown that even cellular extracts removed and purified from PDT treated mice have the ability to induce immunogenic response in untreated mice with tumors. These antigens were found to persist for a period of time lasting up to five weeks following the initial treatment, although their quantities diminished significantly at longer time points. The fact that there does not appear to be a long-term retention of this response may explain why tumors often reoccur. As the levels of the antigens diminish, the immune response also appears to fade, and the conditions regress to their previous states.

During the last two decades, there has been significant research focused on some of the other beneficial effects that photodynamic therapy might produce. Much of the data suggest that photodynamic therapy may lead to damage or destruction of the micro vascular network surrounding diseased tissue.[39, 42-44] This can subsequently lead to hypoxia and anoxia.[45-48] This appears to be the pathway responsible for the beneficial effects of compounds such as psoralen, which is used to treat psoriasis and (to a lesser extent) eczema and vitiligo.

The research described in this thesis is focused on the discovery of new compounds for use in PDT. Towards this end, we have evaluated the photo-induced DNA cleaving abilities of the series of acridine and phenazine-based chromophores shown in Figure 4.
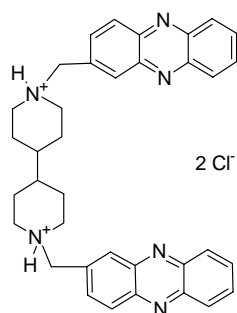
AL-VII-30 (**1**)
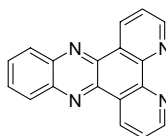
EC-I-12 (**3**)
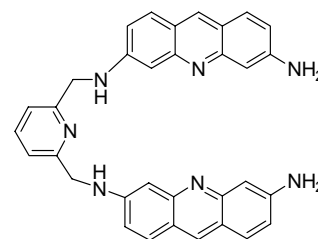
AF-I-50 (**5**)
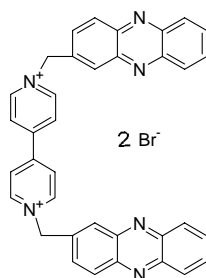
FH-III-165 (**2**)
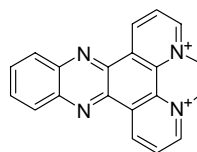
EC-I-13 (**4**)
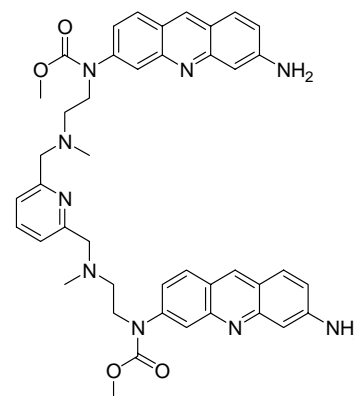
MP-I-73 (**6**)

Figure 4 Investigational Compounds. Compounds were synthesized and character by collaborator Prof. Antonio Lorente *et al.* at the Universidad de Alcalá, Spain. DNA binding and photocleavage by **2** and **6** have been extensively characterized by Dr. Xia Yang and Dr. Beth Wilson, respectively.[52, 53] Partial analyses of **2** and **6** have been included in this thesis for comparison purposes.

The extended, aromatic ring systems of these compounds are expected to intercalate between adjoining base pairs in the DNA double-helix. We have shown that photocleavage of plasmid DNA is achieved at micromolar concentrations of compound under near physiological conditions of pH and temperature (pH 7.0 and 22 °C). The plasmid pUC19 was employed in this study because of its size and availability. This plasmid is an accessory chromosome isolated from the bacterium *Escherichia coli*. The cleaving agent can induce nicks into the supercoiled DNA, which is then transformed to its relaxed or nicked form. The compounds investigated were shown to produce frank

stand breaks in the plasmid DNA, which were visualized by employing nondenaturing agarose gel electrophoresis. The plasmid fragments of linear, supercoiled and nicked forms can be isolated and observed on agarose gels, because the supercoiled plasmid migrates through the gel at a faster rate than the relaxed and linear forms. Photosensitizers can theoretically produce either single-strand breaks (SSBs) or double-strand breaks (DSBs). DSBs typically occur when two SSBs are located within 10 base pairs on opposite strands of the DNA helix.

The photonucleases **3**, **5**, and **6** in Figure 4 were designed to chelate copper(II), which is intended to enhance binding and thereby induce increased levels of DNA photocleavage. This is significant in light of the broad distribution of copper in biological systems.[49, 50]

Methods and Materials

General

Calf thymus DNA (CT-DNA) was obtained from Invitrogen (Lot: 1147749A). The concentrations of the DNA were determined based on the Beer's Law (1),

$$Absorbance \quad = c \, \varepsilon \, l \qquad \textbf{(1)}$$

where c is the concentration of CT-DNA , l represents the path length of the cell (1 cm), and ε_{260}= 12,824 M^{-1} (bp) cm^{-1} for CT-DNA.[51] The measurements were taken in a total volume of 500 μL of ddH_2O. Each of the samples was vortexed to mix and allowed to preequilibrate for 60 min before absorbance was measured. Spectral data on the intercalants were recorded with a UV-1601 UV-Visible Shimadzu Spectrophotometer.

The putative intercalants **1** through **6** (Figure 4) were synthesized in Professor Antonio Lorente's laboratory at the Universidad de Alcalá, Spain. Superoxide dismutase (SOD), catalase, D-mannitol, D-sorbitol, sodium benzoate, sodium azide and ethidium bromide were purchased from Sigma-Aldrich. Agarose was obtained from Fisher Scientific.

DNA photocleavage reactions were conducted in a Rayonet Photochemical Reactor fitted with eleven 24 Watt RPR-350 nm Rayonet lamps (The Southern New England Ultraviolet Company) for phenazine derivatives **1** to **4**, or eight 40 Watt RPR-419 nm Rayonet lamps for the acridine derivatives **5** and **6**. Images of agarose gels were visualized using an UV transilluminator (VWR) set at 302 nm and photographs obtained with a Polaroid DS-43/GelCam camera fitted with type 667 film (VWR).

Large–Scale Plasmid Preparation

A total of 50 μL of competent cells (*E. coli* XL-1 blue, Stratagene) was

transformed with 1 μL pUC19 plasmid DNA (500 ng/ μL; Promega) by heat shocking the

cells for 90 s at 42 ˚C. Next, 1 mL SOB *E. coli* culture media (1 L solution: Bacto

Tryptone 20.0 g, Yeast Extract 5.0 g, NaCl Deionized H_2O 0.5 g, 800.0 ml) was added

and the solution was incubated while shaking at 37 ˚C for 1 h in a 1.5 mL Eppendorf tube.

Two 2% agarose plates were prepared from 100 mL solutions of sterilized Luria-Bertani

(LB) broth inoculated with ampicillin (60 μg/mL). A total of 50 μL of the SOB *E.coli*

culture mixture was streaked onto the surface of each agarose plate. The two culture

plates were incubated overnight at 37 ˚C. A single colony was selected and grown for 8 h

at 37 ˚C in a 2 mL solution of ampicillin inoculated LB broth while shaking on a Labline

shaker. A total of 1 mL of this solution was then added to each of two 500 mL solutions

of the inoculated LB broth and shaken for 16 h on the Labline shaker. The solutions were

then centrifuged at 18,000 rpm for 30 min, and the supernatants removed. Plasmid was

extracted from the recovered cell pellets using a Qiagen Plasmid Maxi kit according to

the manufacturer's instructions. The concentration of the resulting purified DNA was

measured using the Shimadzu UV-1601 spectrophotometer, using the extinction

coefficient $\varepsilon = 12824$ bp·M^{-1}·cm^{-1}. DNA purity was determined based on equation (2). A

ratio value of 1.8 or greater indicated that the DNA plasmid was considered to be free of

protein contamination.[51]

$$Purity = \frac{Abs_{260}}{Abs_{280}} \qquad (2)$$

Gel-Shift Assay

      To determine the concentration at which a dsDNA mobility shift could be detected using agarose gel electrophoresis, increasing concentrations of the four intercalants, **1, 3, 4,** and **5** were mixed with 38.5 µM bp pUC19 DNA in 20 mM sodium phosphate buffer, pH 7.0, in a total volume of 20 µL. The solutions were equilibrated in the dark for 1 h and were then electrophoresed on a 1.0 % non-denaturing agarose gel at 20 mV over 16 h. After electrophoresis, gels were stained with ethidium bromide (0.5 µg/mL), visualized on a transilluminator set at 302 nm, and photographed with a Polaroid Gelcam.

Thermal Melting Studies

      Thermal denaturation experiments were conducted using 30 µM bp of CT-DNA at a [compound]/[DNA] molar ratio of 0.5 in 20 mM phosphate buffer pH 7.0 using compounds **3**, **4**, and **5**. (Compound **1** was excluded from this analysis due to thermal degradation above 60 ˚C.) All solutions were in a total volume of 3 mL prepared in 3 mL quartz cuvettes (Starna). Samples were equilibrated in dark for 1 h at room temperature then heated from 25 ˚C to 100 ˚C at a rate of 0.5 ˚C / min using a Peltier heat block, while the absorbance was monitored at 260 nm.

      The absorbance data was normalized using the equation $A_{normailized} = (A_{\text{CT-DNA}} - A_{lowest})/(A_{highest} - A_{lowest})$. The normalized absorbance was then plotted as a function of temperature and the melting temperature was then determined from the maximum of the first-derivative plot. A change in the T_m was calculated based on the formula $\Delta T_m = T_m$ $_{(\text{CT-DNA + Compound})} - T_m$ $_{(\text{CT-DNA})}$. All data sets were processed using KaleidaGraph™ Version 3.5 software.

Photocleavage Cleavage of dsDNA

Typical reaction conditions involved 38.5 μM bp pUC19 dsDNA plasmid, 20 mM sodium phosphate buffer pH 7.0, and micromolar concentrations of halogen salts of intercalants in a total volume of 20 μL. The solutions were preequilibrated in the dark for 1 h and were then were irradiated at room temperature under aerobic conditions in a ventilated Rayonet Photochemical Reactor. Irradiation wavelengths were selected based on the λ_{max} of each compound. Parallel reactions without compound and/or irradiation were run as controls. The reactions were then mixed with 3 μL of an aqueous loading buffer (0.25% xylene cyanol FF, 0.25% bromophenol blue, 15% Ficoll Type 400) and electrophoresed at 4 V/cm on a 1.0% agarose gel for 90 min. The TAE buffer solution contained ethidium bromide (0.5 μg/mL). Gel images were captured with a Polaroid Gelcam and then quantified with a Molecular Dynamics FluorImager SI Gel Imaging System (Molecular Dynamics). Background corrections were done through a local averaging method. To adjust for the decreased binding of ethidium bromide to supercoiled DNA as compared to the nicked and linear forms, the following formulae, **3** and **4**, were employed to calculate cleavage yields.[51]

$$\% \ Supercoiled \ DNA = \frac{1.22 \ * Volume \ of \ Supercoiled \ DNA}{Volume \ of \ nicked \ DNA \ + \ 1.22 \ * \ Volume \ of \ Supercoiled \ DNA} \ * 100 \qquad \textbf{(3)}$$

$$\% \ Nicked \ DNA \ = \frac{Volume \ of \ nicked \ DNA}{Volume \ of \ nicked \ DNA \ + \ 1.22 \ * \ Volume \ of \ Supercoiled \ DNA} \ * 100 \qquad \textbf{(4)}$$

Concentration Profile Experiments

A series of 20 μL reactions was prepared containing 38.5 μM bp pUC19 DNA, 20 mM sodium phosphate buffer pH 7.0, and increasing concentrations of halogen salts of intercalants **1**, **2**, **3**, **4**, **5** and **6**. The samples were equilibrated in the absence of light for 60 min and irradiated for 60 min at room temperature in a ventilated Rayonet Photochemical Reactor. Reaction products were resolved on a 1.0 % non-denaturing agarose gel and quantitated as described above. The DNA photocleavage conversion was calculated based on cleavage yields obtained in parallel reactions without irradiation using the equations **3** and **4**.

Time Course Profile Experiments

A series of 20 μL reactions was prepared containing 38.5 μM bp pUC19 DNA, 20 mM sodium phosphate buffer pH 7.0, and optimal concentrations of halogen salts of intercalants **1**, **3**, **4**, **5** and **6**. The samples were incubated in the absence of light for 1 h and irradiated for time periods from 0 to 60 min in 10 min increments at room temperature in a ventilated Rayonet Photochemical Reactor. Reaction products were resolved on a 1.0 % non-denaturing agarose gel and quantitated as described above using equations **3** and **4**.

Scavenger Experiments

A series of 20 μL reactions was prepared containing 38.5 μM bp pUC19 DNA, 20 mM sodium phosphate buffer pH 7.0, and micromolar concentrations of halogen salts of intercalants **1**, **2**, **3**, **4**, **5** and **6**. The samples were incubated in the absence of light for 1 h and irradiated in the presence of either 100 mM sodium azide, 100 mM sodium benzoate, 50 units superoxide dismutase, 50 units catalase, 20 mM D-sorbitol, or 20 mM D-mannitol for 50 min at room temperature in a ventilated Rayonet Photochemical Reactor.

Reaction production were resolved on a 1.0 % non-denaturing agarose gel and quantitated as described above. The percent inhibition of DNA photocleavage was calculated based on cleavage yields obtained in parallel reaction run without scavenger using equations **3**, **4**, and **5**.

$$\% \ Inhibition \ = \frac{\% \ cleavage \ w/compound \ - \% \ cleavage \ w/compound \ and \ scavenger}{\% \ cleavage \ w/compound \ - \% \ cleavage \ light \ only} * 100 \quad \textbf{(5)}$$

Salt Inhibition Experiments

A series of 20 μL reactions was prepared containing 38.5 μM bp pUC19 DNA, 20 mM sodium phosphate buffer pH 7.0, and micromolar concentrations of halogen salts of intercalants **1**, **2**, **3**, **4**, **5** and **6** and 0 to 150 mM NaCl. The samples were incubated in the absence of light for 1 h and then were irradiated for 60 min at room temperature in a ventilated Rayonet Photochemical Reactor. Reaction products were resolved on a 1.0% non-denaturing agarose gel and quantitated as described above. The percent inhibition of DNA photocleavage was calculated based on cleavage yields obtained in parallel reaction run without salt using equations **3**, **4**, and **6**.

$$\% \ Inhibition \ = \frac{\left(reaction \ w/o \ NaCl - background \right) - \left(reaction \ w/NaCl - background \right)}{\left(reaction \ w/o \ NaCl - cleavage \ light \ only \right)} * 100 \quad \textbf{(6)}$$

Results and Discussion

DNA Binding Studies

UV-Vis Spectrophometry

  The λ_{max} of each of the compounds **1** to **6** was determined using 1 mM stock solutions of the putative intercalators, which were diluted to reach final concentrations of 50 µM in a volume of 500 µL. Each of these solutions was equilibrated for 1 h, after which absorption spectra were recorded (Table 2; Figures 5 to 10).

Compound	λ_{max} (nm)	Abs @ λ_{max} (mOD)	λ_{max} w/ CT-DNA (nm)	Abs @ λ_{max} w/ CT-DNA (mOD)
1	371	873	365	500
2	371	1704	371	985
3	362	23 [1, 2]	363	25 [2]
4	364	622	364	507
5	437	1451	451	1246
6	452	488	462	414

 Table 2 UV-Vis Absorption Data. Solutions of 50 µM of compound with and without 10 µM calf-thymus DNA were prepared in ddH$_2$O and were incubated for 1 h in absence of light. Absorption spectra were acquired using a Shimadzu UV-1601 Spectrophotometer.
[1] EC-1-12 absorbance obtained in the presence of 1.0 % SDS: λ_{max} = 362 nm, Abs @ λ_{max} = 653 mOD .
[2] EC-1-12 absorbance in table is very low due to possible aggregation of compound.

  Compounds **1**, **2**, **4**, **5** and **6** showed a marked decrease in absorbance upon the addition of CT-DNA (Table 2). This may be indicative of the compounds binding to

DNA. In addition, compounds **5**, and **6** showed evidence of pronounced bathochromic shifts in their λ_{max} values. This provides evidence supporting intercalation as a possible binding mode for these compounds. The absorbance of compound **3** was also recorded in the presence of 1.0 % SDS to disrupt aggregation. Thus, the absorbance at 362 nm the absence of SDS is significantly lower due to aggregation of the compound in buffer. When DNA is added, absorbance at 362 nm is unchanged.
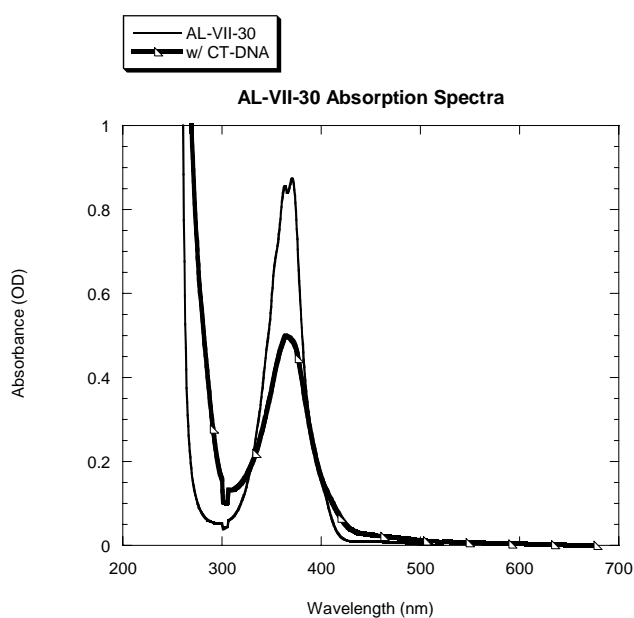
Figure 5 UV-vis Absorption Spectra of Al-VII-30, Compound 1. Two 50 μM solutions of compound **1,** one in ddH$_2$O only and one with 10 μM CT-DNA in ddH$_2$O, were incubated for 1 h in the absence of light.
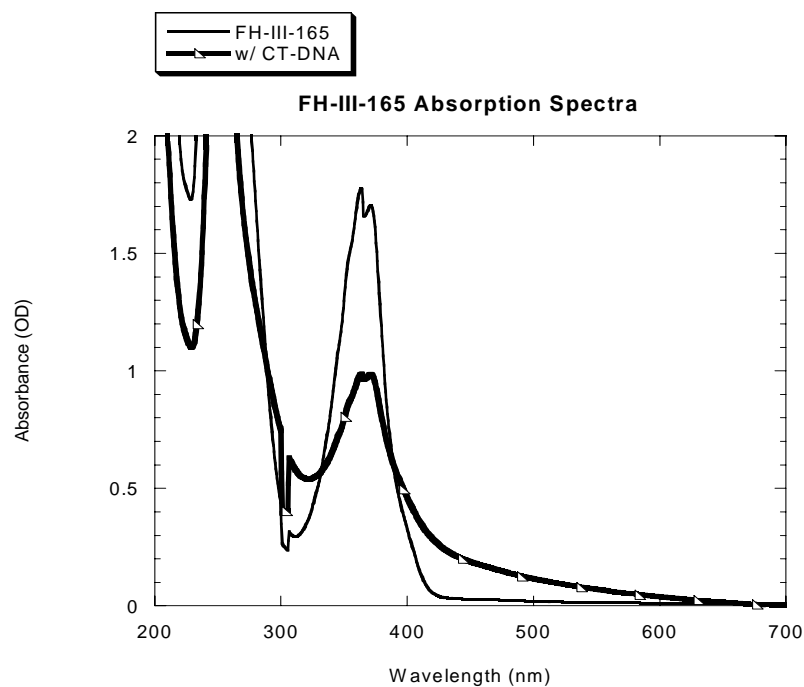
Figure 6 UV-vis Absorption Spectra of FH-III-165, Compound 2. Two 50 μM solutions of compound **2**, one in ddH$_2$O only and one with 10 μM CT-DNA in ddH$_2$O, were incubated for 1 h in the absence of light.
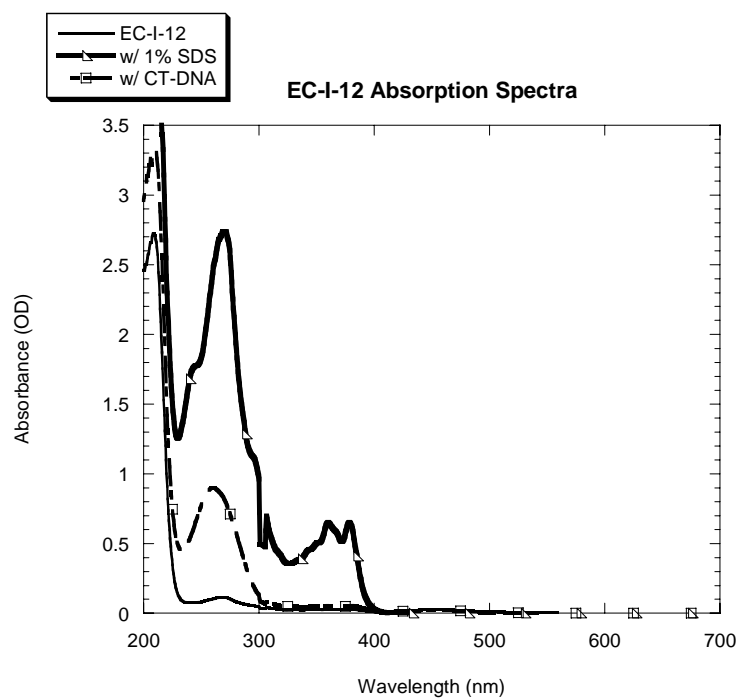
Figure 7 UV-vis Absorption Spectra of EC-I-12, Compound 3. Three 50 μM solutions of compound **3**, one in ddH$_2$O only, one containing 1% SDS and one with 10 μM CT-DNA in ddH$_2$O, were incubated for 1 h in the absence of light.

24
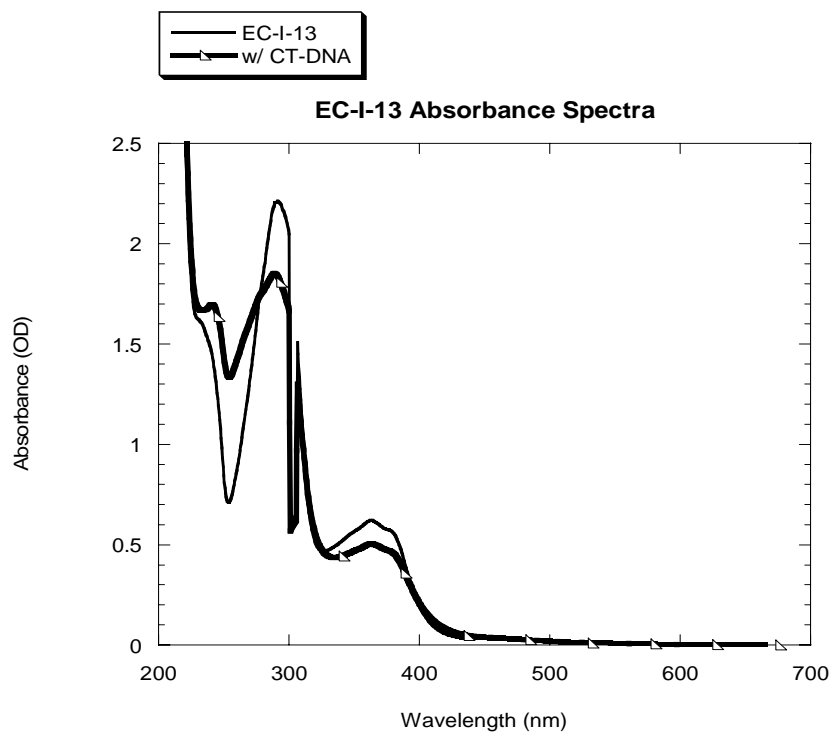
Figure 8 UV-vis Absorption Spectra of EC-I-13, Compound 4. Two 50 μM solutions of compound **4**, one in ddH$_2$O only and one with 10 μM CT-DNA in ddH$_2$O, were incubated for 1 h in the absence of light.
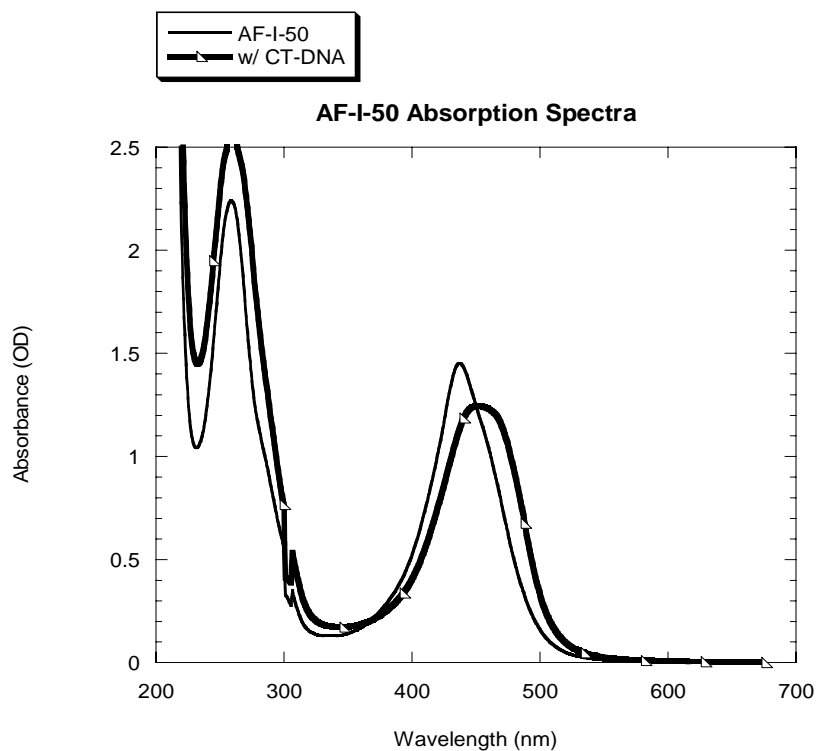
Figure 9 UV-vis Absorption Spectra of AF-I-50, Compound 5. Two 50 μM solutions of compound **5**, one in ddH$_2$O only and one with 10 μM CT-DNA in ddH$_2$O, were incubated for 1 h in the absence of light.
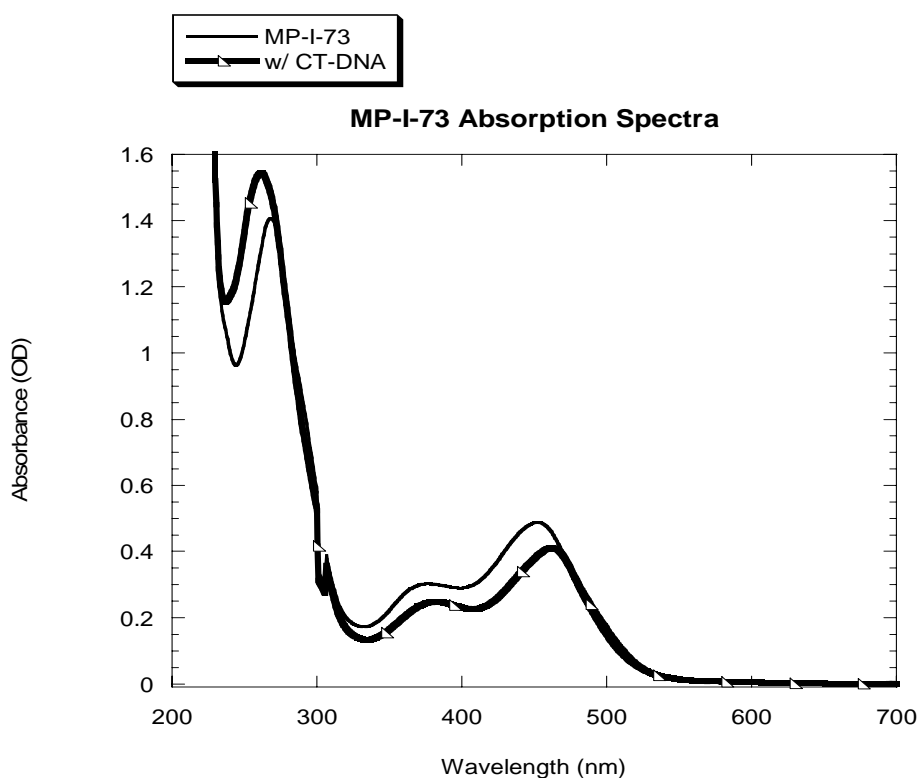
Figure 10 UV-vis Absorption Spectra of MP-I-73, Compound 6. Two 50 μM solutions of compound **6**, one in ddH$_2$O only and one with 10 μM CT-DNA in ddH$_2$O,were incubated for 1 h in the absence of light.

Thermal Melting Assay

Thermal denaturation experiments were conducted for the putative intercalants **3**, **4**, and **5**, using 38.5 μM bp of CT-DNA at a [compound]/[DNA] molar ratio of 0.5 in 20 mM phosphate buffer pH 7.0 (Figures 11 to 13). (Compound **1** was excluded from this analysis due to thermal degradation observed above 60 ˚C.) Absorbance at 260 nm was measured as a function of increasing temperature. The temperature was raised from 25 to 100 ˚C at a rate of 0.5 ˚C per min with a Peltier block. Normalized absorbance was then plotted as a function of temperature and the melting temperature was then determined from the maxima of first-derivative plots. A change in the T_m of CT-DNA upon the addition of compound was calculated based on the equation $\Delta T_m = T_{m\,(\text{CD-DNA + Cmpd})} - T_{m\,(\text{CT-DNA})}$. When a compound binds to double-helical DNA, the helix is usually stabilized

26

and the melting temperature increases as a function of the binding affinity of the

compound. Therefore, the results of the T_m data suggest that the compounds bind to DNA

with decreasing affinity as follows: **2 > 4 > 5 > 6 w/Cu(II) > 6 w/o Cu(II) > 3** (Table **3**).
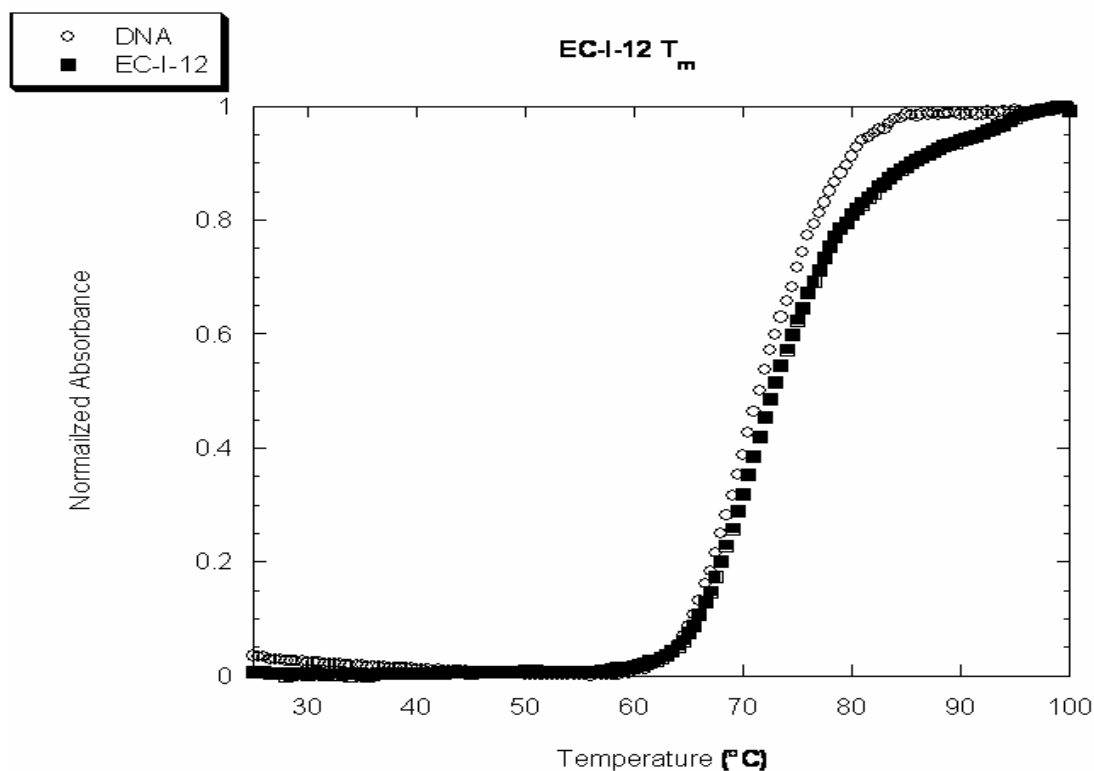
Figure 11 Thermal Melting Assay EC-I-12, Compound 3. Experiments employed 38.5 µM bp of CT-DNA at a [compound **3**]/[DNA bp] molar ratio of 0.5 in 20 mM phosphate buffer pH 7.0. After incubation in dark for 2 h, the samples were heated from 25 °C to 100 °C at a rate of 0.5 °C / min using a Peltier heat block, while the absorbance was monitored at 260 nm.
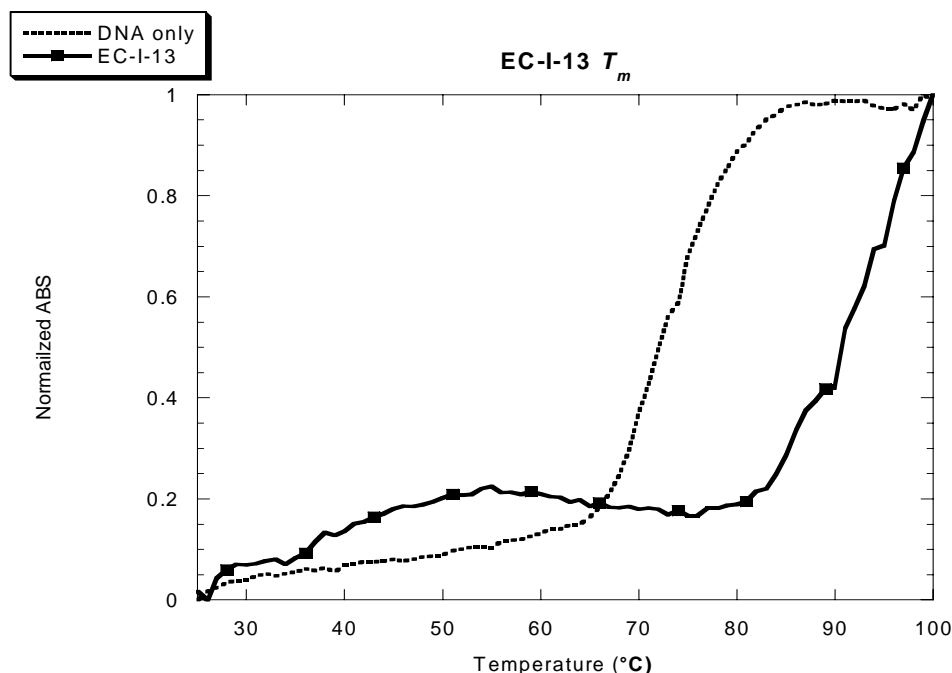
Figure 12 Thermal Melting Assay EC-I-13, Compound 4. Experiments employed 38.5 µM bp of CT-DNA at a [compound **4**]/[DNA bp] molar ratio of 0.5 in 20 mM phosphate buffer pH 7.0. After incubation in dark for 2 h, the samples were heated from 25 ˚C to 100 ˚C at a rate of 0.5 ˚C / min using a Peltier heat block, while the absorbance was monitored at 260 nm.
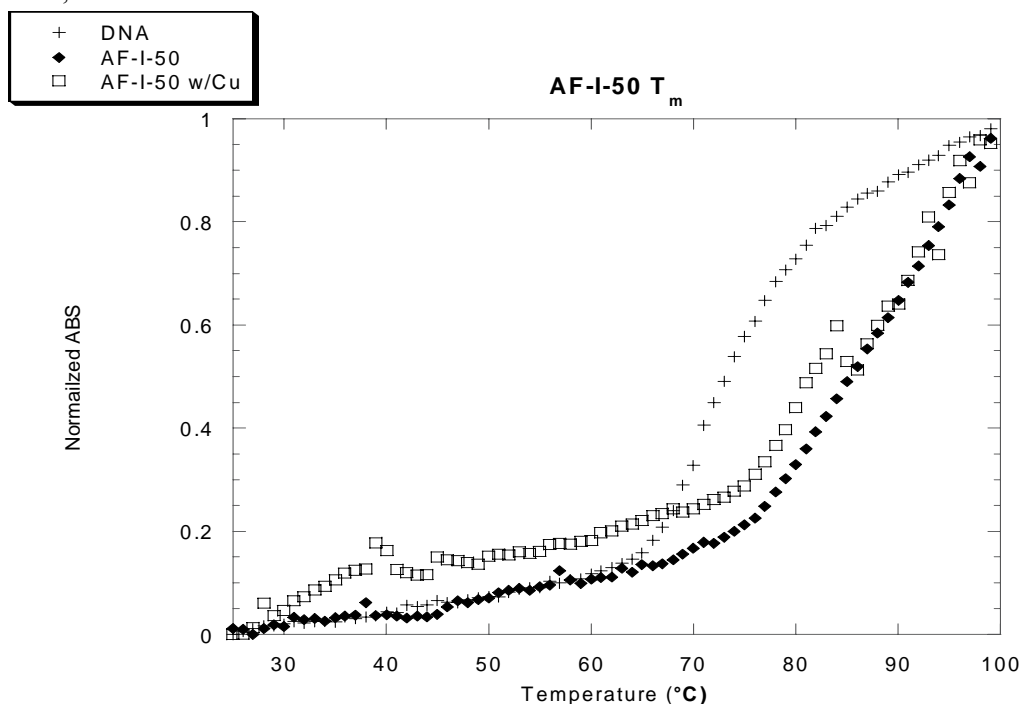
Figure 13 Thermal Melting Assay AF-I-50, Compound 5. Experiments employed 38.5 µM bp of CT-DNA at a [compound **5**]/[DNA bp] molar ratio of 0.5 in 20 mM phosphate buffer pH 7.0, in the presence (♦) and absence (□)of equimolar CuCl₂. After incubation in dark for 2 h, the samples were heated from 25 ˚C to 100 ˚C at a rate of 0.5 ˚C / min using a Peltier heat block, while the absorbance was monitored at 260 nm.

28

Compound (0.5 compound/DNA ratio)	ΔT_m (˚C)
AL-VII-30 (**1**)	N/A
FH-III-165 [1] (**2**)	26
EC-I-12 (**3**)	3
EC-I-13 (**4**)	22
AF-I-50 (**5**)	15
MP-I-73 [2] (**6**)	4; 10 [w/ Cu(II)]

Table 3 Thermal Melting Assay. Experiments employed 38.5 µM bp of CT-DNA at a [compound]/[DNA] molar ratio of 0.5 in 20 mM phosphate buffer pH 7.0 using compounds: AF-I-50, EC-I-12, EC-I-13. Samples were heated from 25 ˚C to 100 ˚C at a rate of 0.5 ˚C / min using a Peltier heat block, while the absorbance was monitored at 260 nm.
[1] Data obtain by Xia Yang at 10 mM potassium phosphate buffer pH 7.0 in the presence of 37.5 µM CT-DNA and 0.5 molar ratio [drug]/[DNA].[52]
[2] Data obtained by Beth Wilson at 20 mM sodium phosphate buffer pH 7.1 in the presence of 10 µM **6**, and 15 µM bp CT-DNA. [53]

Gel Mobility Shift Assay

Intercalators stack in between the adjacent base pairs within the DNA molecule, causing it to unwind and extend its compact, double-helical structure. This extension in the strand length reduces the mobility of the DNA as it migrates through agarose gels. The behavior is usually characteristic of intercalating molecules. Molecules which bind to the grooves of DNA do not usually cause significant increases in strand length. Therefore, smaller changes in migration are typically observed.

In the DNA mobility experiments described in this thesis, increasing concentrations of compound were equilibrated with DNA in the dark for 1 h and then

subjected to electrophoresis on 1.0 % agarose gels under low voltage. After being

allowed to migrate for 24 h, the agarose gels were stained with ethidium bromide, and

visualized with a UV transilluminator. The gels were then photographed with a Polaroid

Gelcam. Notable shifts were observed for compounds **1**, **4** and **5** (Figures 14, 16, and 17-

18), while no shift was seen in the case of compound **3** (Figure 15). The most significant

shift was produced by compound **5,** which was followed by compound **4** and then **1**. It is

worth mentioning that compound **5** displayed significant bathochromicity and

hypochromicity (Table 2, Figure 9) and produced a significant increase in the T_m (Table 3,

Figure 13) upon binding to DNA.
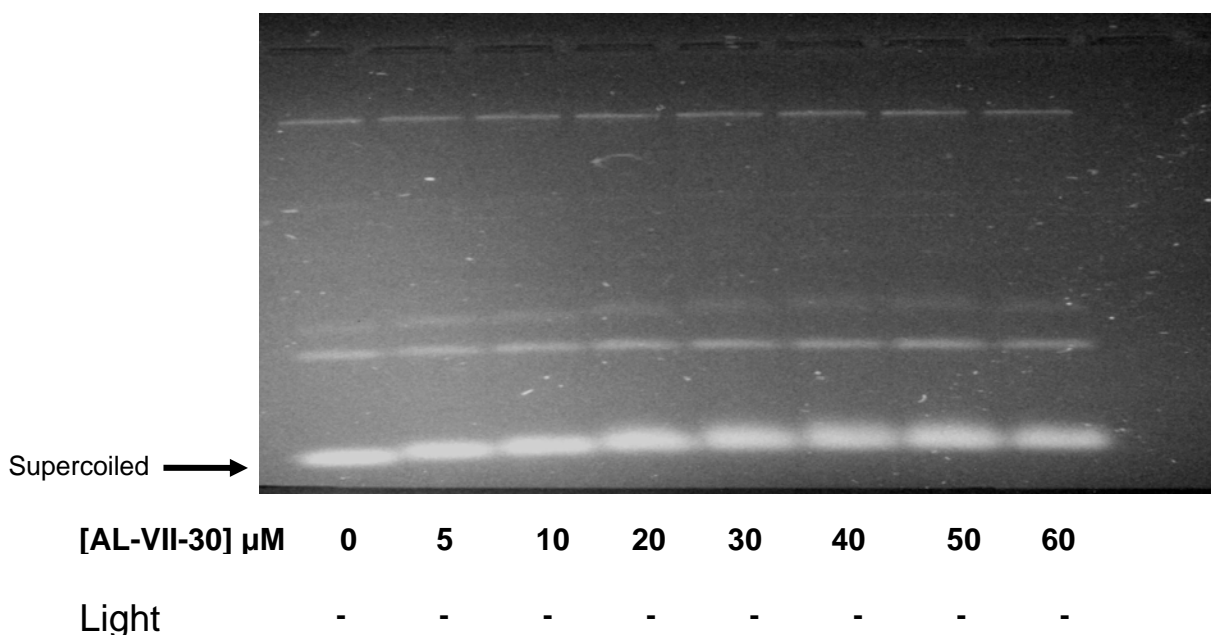
Figure 14 Gel Mobility Assay, AL-VII-30, Compound 1. Each of the samples was prepared in the presence of 20 mM sodium phosphate buffer pH 7.0 and 38.5 µM bp pUC19 DNA in a 20 µL reaction volume. The samples were allowed to preequilibrate at room temperature for 60 min and then were resolved by agarose gel electrophoresis over 24 h and stained with ethidium bromide for 1 h.

Supercoiled →

EC-I-12 (µM)	0	1	2	4	8	15	30	60	100	200	0
Light	-	-	-	-	-	-	-	-	-	-	-
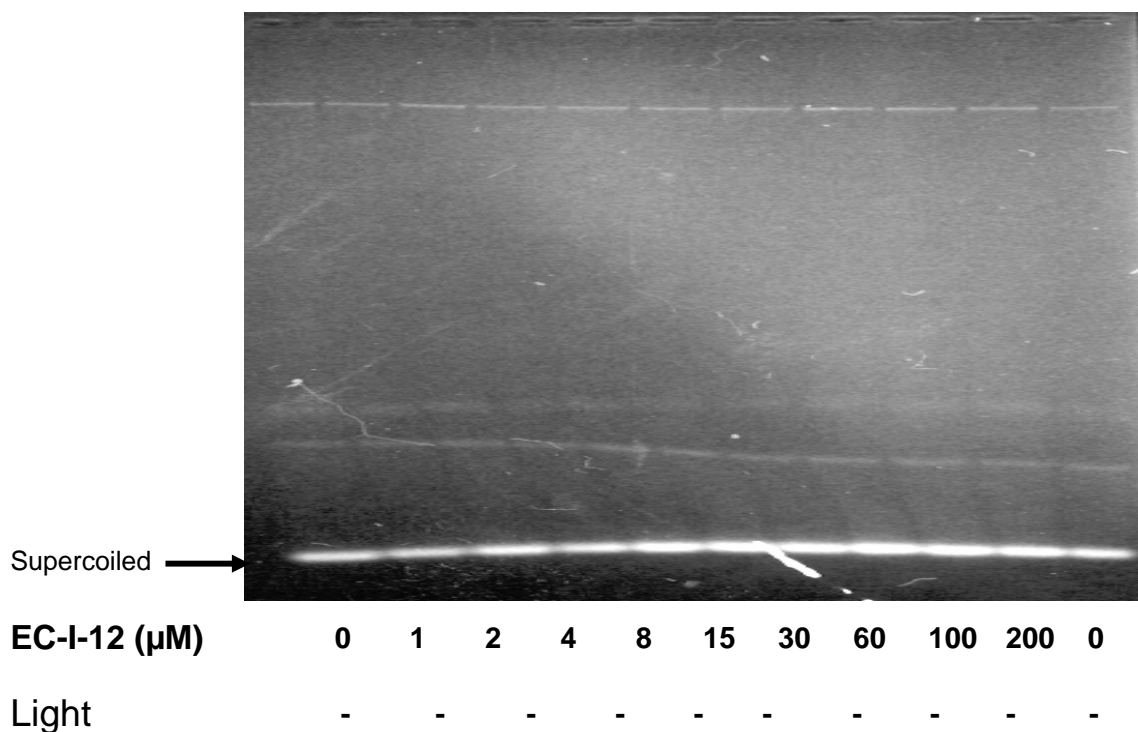
Figure 15 Gel Mobility Assay, EC-I-12, Compound 3. Each of the samples was prepared in the presence of 20 mM sodium phosphate buffer pH 7.0 and 38.5 µM bp pUC19 DNA in a 20 µL reaction volume. The samples were allowed to preequilibrate at room temperature for 60 min and then were resolved by agarose gel electrophoresis overnight and stained with ethidium bromide for 1 h.

Supercoiled →

EC-I-13 (µM)	0	1	2	4	8	15	30	60	100	200	0
Light	-	-	-	-	-	-	-	-	-	-	-
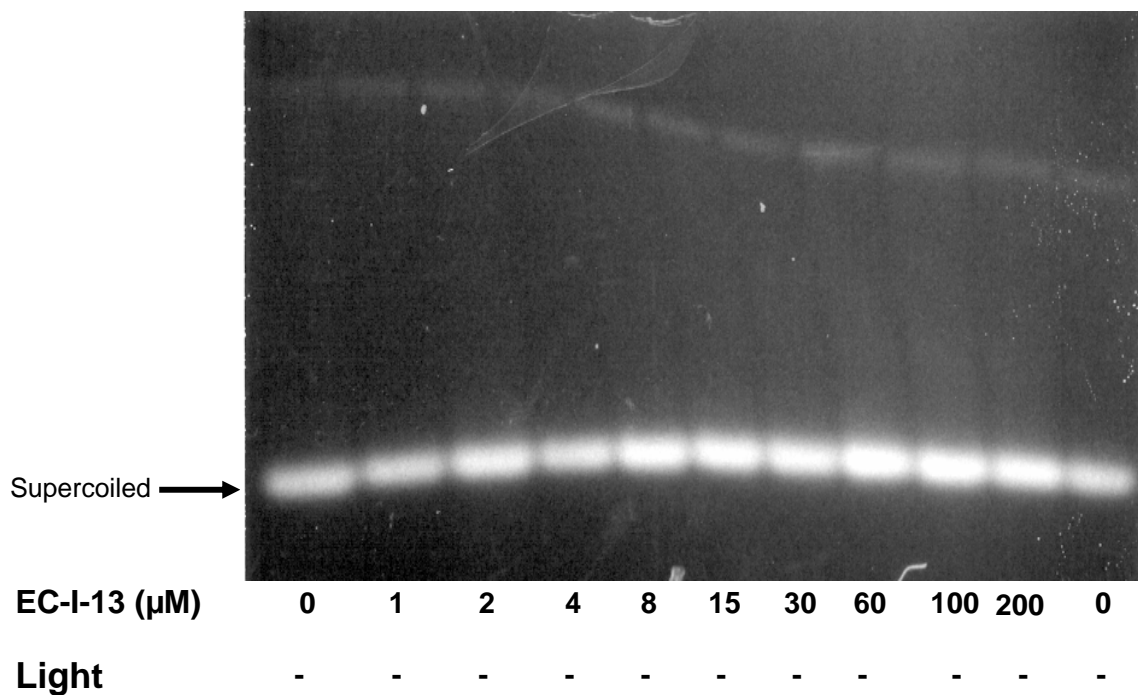
Figure 16 Gel Mobility Assay, EC-I-13, Compound 4. Each of the samples was prepared in the presence of 20 mM sodium phosphate buffer pH 7.0 and 38.5 µM bp pUC19 DNA in a 20 µL reaction volume. The samples were allowed to preequilibrate at room temperature for 60 min and then were resolved by agarose gel electrophoresis overnight and stained with ethidium bromide for 1 h.

31
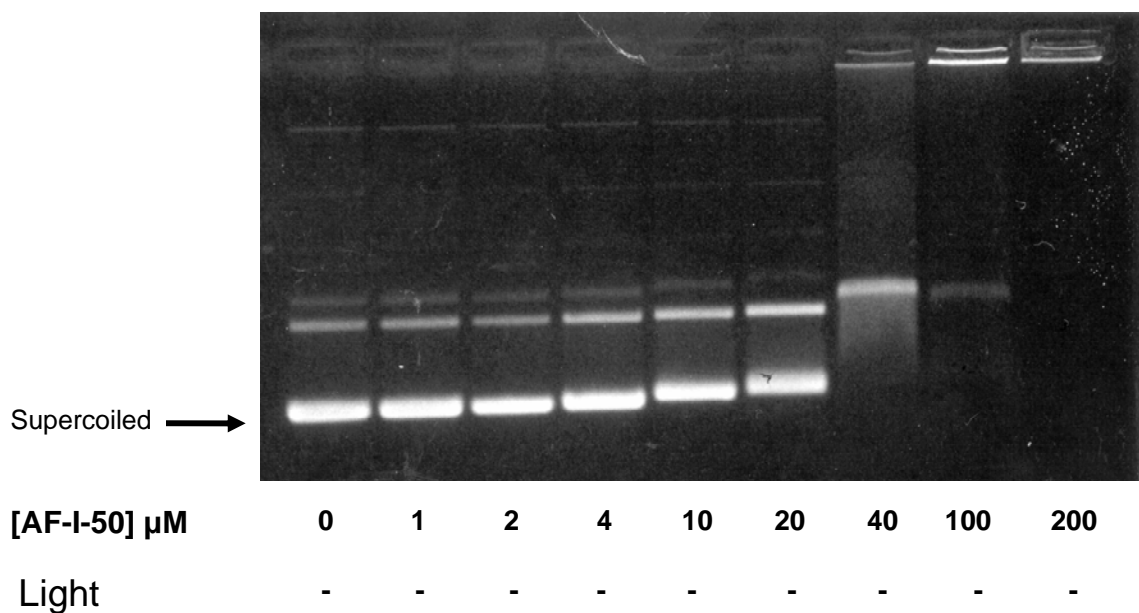
Figure 17 Gel Mobility Assay, AF-I-50, Compound 5 Broad Titration. Each of the samples was prepared in the presence of 20 mM sodium phosphate buffer pH 7.0 and 38.5 µM bp pUC19 DNA in a 20 µL reaction volume. The samples were allowed to preequilibrate at room temperature for 60 min and then were resolved by agarose gel electrophoresis over 24 h and stained with ethidium bromide for 1 h.
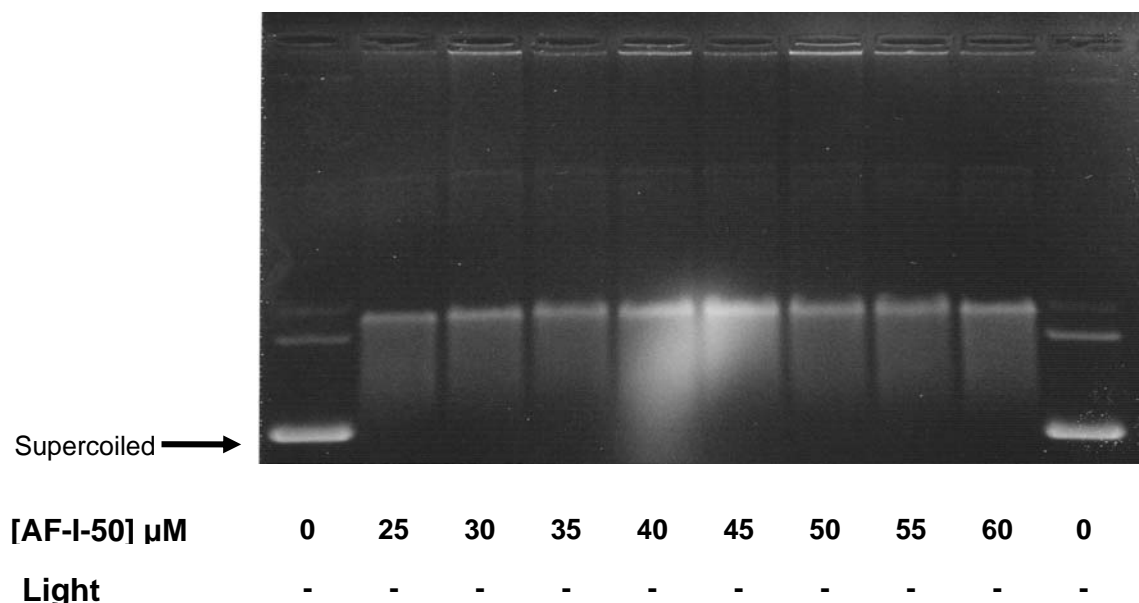
Figure 18 Gel Mobility Assay, AF-I-50, Compound 5 Narrow Titration. Each of the samples was prepared in the presence of 20 mM sodium phosphate buffer pH 7.0 and 38.5 µM bp pUC19 DNA in a 20 µL reaction volume. The samples were allowed to preequilibrate at room temperature for 60 min and then were resolved by agarose gel electrophoresis overnight and stained with ethidium bromide for 1 h.

32

Photocleavage of pUC19 dsDNA, Concentration Titrations

Once the λ_{max} value of each compound had been determined, concentration

evaluation experiments were conducted. The reaction mixtures contained a total volume

of 20 µL and were prepared with 38.5 µM bp of pUC19 plasmid, 20 mM sodium

phosphate buffer pH 7.0, and variable concentrations of compound. These experiments

were conducted to determine the lowest concentration of each compound which was

capable of achieving greater than or equal to 90% conversion of supercoiled plasmid to

either the nicked and/or linear forms (Figure 19 to Figure 27). A summary of the results

is shown in Table 4. For compounds **1 – 4,** the Rayonet Photochemical Reactor was

equipped with eleven 24 Watt RPR-350 nm Rayonet lamps, whereas, in the case of

reactions involving compounds **5** and **6**, and eight 40 Watt RPR-419 nm Rayonet lamps

were used. (The lamps were selected because their emission profiles strongly overlapped

the absorption bands of the compounds being evaluated.)

Compounds **3, 5**, and **6** contain copper binding units. Therefore, each of these

compounds was examined in the presence and absence of 1:1 ratios of copper(II). (Higher

ratios of Cu(II) to compound were not found to provide any additional cleavage

enhancement, while less enhancement was observed at lower ratios of Cu(II) to

compound.) These experiments revealed that compounds **3**, **5** and **6** all showed

significant enhancements in the conversion of supercoiled pUC19 DNA into linear and

nicked forms when irradiated in the presence of Cu(II) (Figure 22, 25, and 27).

Compound	λ_{max} (nm)	Minimum Con. (μM)	w/ Copper(II) (μM)
AL-VII-30 (**1**)	371	4	N/A
FH-III-165 (**2**)	371	0.4	N/A
EC-I-12 (**3**)	362	40	20
EC-I-13 (**4**)	364	8	N/A
AF-I-50 (**5**)	437	5	5
MP-I-73 (**6**)	452	>100	50

Table 4 Concentration Minima. Minimum concentration of compounds required to produce $\geq 90\%$ conversion of supercoiled pUC19 plasmid to nicked/linear forms. Compounds **1-4** were irradiated with eleven 350 nm lamps, while **5** and **6** were irradiated with eight 419 nm lamps. Each of the samples was prepared in the presence of 20 mM sodium phosphate buffer pH 7.0 and 38.5 μM bp pUC19 DNA, in a 20 μL reaction volume. The samples were allowed to preequilibrate at room temperature for 60 min and then were irradiated for 60 min in a ventilated Rayonet Photochemical Reactor under aerobic conditions.

nicked									
linear									
supercoiled									
AL-VII-30 (μM)	0	0	1	2	4	6	7.5	10	20	20
Light	-	+	+	+	+	+	+	+	+	-
% Cleavage	18	21	39	52	96	99	100	100	99	8

Figure 19 Concentration Titration, AL-VII-30, Compound 1. Minimum concentration of compound **1** required for $\geq 90\%$ conversion of supercoiled pUC19 plasmid to nicked/linear forms. Samples were irradiated with eleven 350 nm lamps. Each of the samples was prepared in the presence of 20 mM sodium phosphate buffer pH 7.0 and 38.5 μM bp pUC19 DNA, in a 20 μL reaction volume. The samples were allowed to preequilibrate at room temperature for 60 min and then were irradiated for 60 min in a ventilated Rayonet Photochemical Reactor under aerobic conditions.

FH-III-165 (µM)	0	0.1	0.2	0.4	0.6	0.8	1.0	1.2	1.4	1.4
Light	-	+	+	+	+	+	+	+	+	-
% Cleavage	7	56	72	91	96	97	98	97	99	6
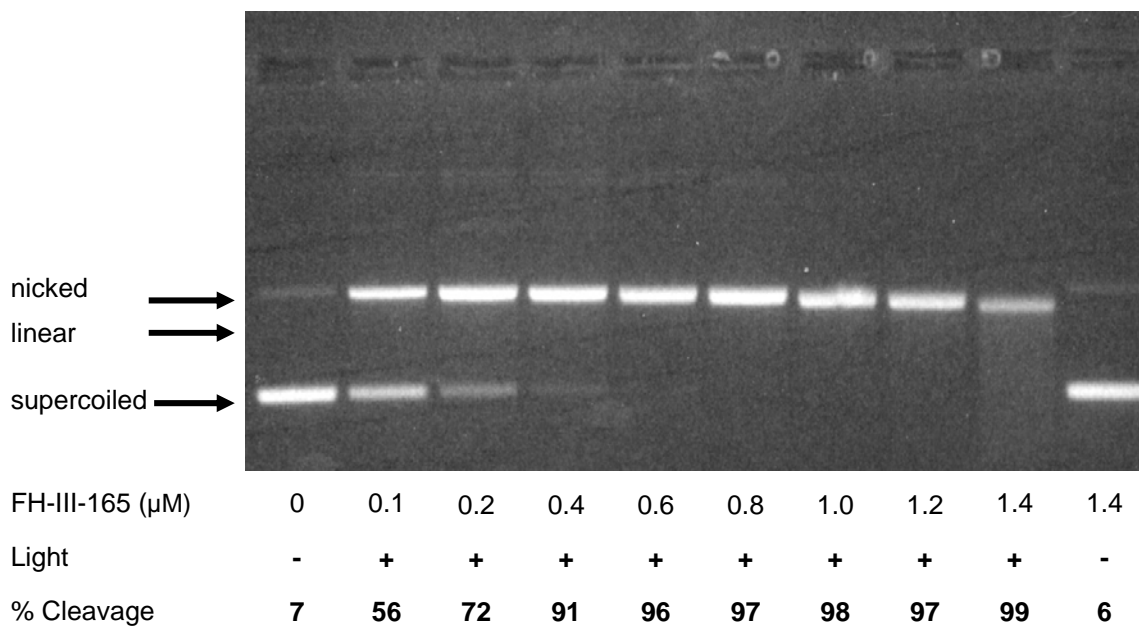
Figure 20 Concentration Titration, FH-III-165, Compound 2. Minimum concentration of compound **2** required for ≥ 90% conversion of supercoiled pUC19 plasmid to nicked/linear forms. Samples were irradiated with eleven 350 nm lamps. Each of the samples was prepared in the presence of 20 mM sodium phosphate buffer pH 7.0 and 38.5 µM bp pUC19 DNA, in a 20 µL reaction volume. The samples were allowed to preequilibrate at room temperature for 60 min and then were irradiated for 60 min in a ventilated Rayonet Photochemical Reactor under aerobic conditions.

EC-I-12 (µM)	0	10	20	30	40	50	60	70	70
CuCl$_2$	-	-	-	-	-	-	-	-	-
Light	+	+	+	+	+	+	+	+	-
% cleavage	18	31	73	82	92	98	97	99	4

Figure 21 Concentration Titration, EC-I-12 w/o Cu(II), Compound 3. Minimum concentration of compound **3** required for ≥ 90% conversion of supercoiled pUC19 plasmid to nicked/linear forms. Samples were irradiated with eleven 350 nm lamps. Each of the samples was prepared in the presence of 20 mM sodium phosphate buffer pH 7.0 and 38.5 µM bp pUC19 DNA, in a 20 µL reaction volume. The samples were then allowed to preequilibrate at room temperature for 60 min and then were irradiated for 60 min in a ventilated Rayonet Photochemical Reactor under aerobic conditions.

nicked											
linear											
supercoiled											
EC-I-12 (µM)	0	0	10	20	30	40	50	60	70	80	80
CuCl₂	+	+	+	+	+	+	+	+	+	+	+
Light	-	+	+	+	+	+	+	+	+	+	-
% cleavage	18	34	85	90	94	91	97	96	98	100	19

Figure 22 Concentration Titration, EC-I-12 w/Cu(II), Compound 3. Minimum concentration of compound **3** required for ≥ 90% conversion of supercoiled pUC19 plasmid to nicked/linear forms in the presence of 1:1 molar equivalents of Cu(II). Samples were irradiated with eleven 350 nm lamps. Each of the samples was prepared in the presence of 20 mM sodium phosphate buffer pH 7.0 and 38.5 µM bp pUC19 DNA, in a 20 µL reaction volume. The samples were allowed to preequilibrate at room temperature for 60 min and then were irradiated for 60 min in a ventilated Rayonet Photochemical Reactor under aerobic conditions.

nicked									
linear									
supercoiled									
EC-I-13 (µM)	0	0	1	2	4	8	15	30	60	60
Light	-	+	+	+	+	+	+	+	+	-
% cleavage	11	26	46	55	73	93	96	97	99	10

Figure 23 Concentration Titration EC-I-13, Compound 4. Minimum concentration of compound **4** required for ≥ 90% conversion of supercoiled pUC19 plasmid to nicked/linear forms. Samples were irradiated with eleven 350 nm lamps. Each of the samples was prepared in the presence of 20 mM sodium phosphate buffer pH 7.0 and 38.5 µM bp pUC19 DNA, in a 20 µL reaction volume. The samples were allowed to preequilibrate at room temperature for 60 min and then were irradiated for 60 min in a ventilated Rayonet Photochemical Reactor under aerobic conditions.

36

nicked										
linear										
supercoiled										
AF-I-50 (µM)	0	0	5	10	20	30	40	50	60	60
CuCl$_2$	-	-	-	-	-	-	-	-	-	-
Light	-	+	+	+	+	+	+	+	+	-
% cleavage	11	10	96	94	94	96	96	98	99	4

Figure 24 Concentration Titration, AF-I-50, Compound 5. Minimum concentration of compound **5** required for ≥ 90% conversion of supercoiled pUC19 plasmid to nicked/linear forms. Samples were irradiated with eight 419 nm lamps. Each of the samples was prepared in the presence of 20 mM sodium phosphate buffer pH 7.0 and 38.5 µM bp pUC19 DNA, in a 20 µL reaction volume. The samples were allowed to preequilibrate at room temperature for 60 min and then were irradiated for 60 min in a ventilated Rayonet Photochemical Reactor under aerobic conditions.
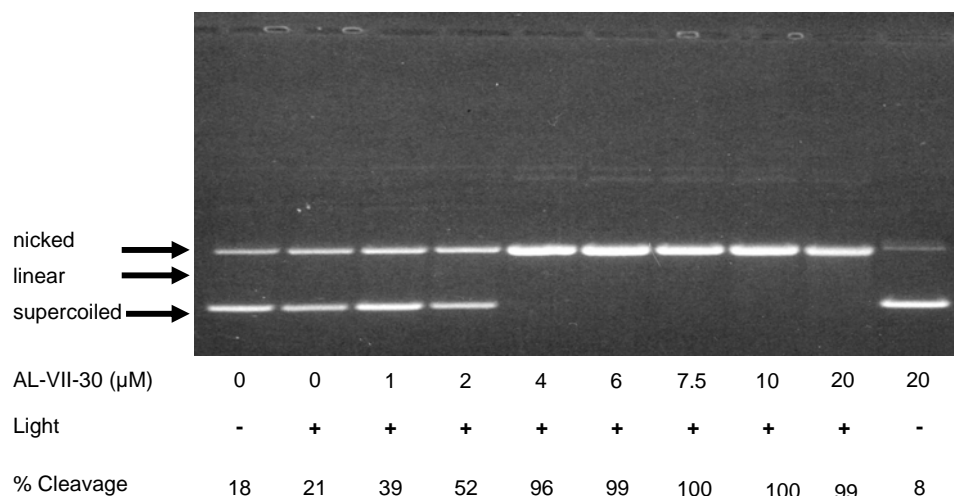

nicked										
linear										
supercoiled										
AF-I-50 (µM)	0	0	1	2	4	5	6	10	20	40	40
CuCl$_2$	+	+	+	+	+	+	+	+	+	+	+
Light	-	+	+	+	+	+	+	+	+	+	-
% cleavage	4	18	50	62	83	91	96	99	100	100	7

Figure 25 Concentration Titration, AF-I-50 w/CuCl$_2$. Minimum concentration of compound **5** required for ≥ 90% conversion of supercoiled pUC19 plasmid to nicked/linear forms in the presence of equimolar copper(II). Samples were irradiated with eight 419 nm lamps. Each of the samples was prepared in the presence of 20 mM sodium phosphate buffer pH 7.0 and 38.5 µM bp pUC19 DNA, in a 20 µL reaction volume. The samples were allowed to preequilibrate at room temperature for 60 min and then were irradiated for 60 min in a ventilated Rayonet Photochemical Reactor under aerobic conditions.

37

MP-I-73 (µM)	0	0	10	20	30	40	50	60	70	70
$CuCl_2$	-	-	-	-	-	-	-	-	-	-
Light	-	+	+	+	+	+	+	+	+	-
% cleavage	9	15	42	40	41	41	40	40	45	12

Figure 26 Concentration Titration, MP-I-73, Compound 6. Minimum concentration of compound **6** required for ≥ 90% conversion of supercoiled pUC19 plasmid to nicked/linear forms in the absence of copper(II). Samples were irradiated with eight 419 nm lamps. Each of the samples was prepared in the presence of 20 mM sodium phosphate buffer pH 7.0 and 38.5 µM bp pUC19 DNA, in a 20 µL reaction volume. The samples were allowed to preequilibrate at room temperature for 60 min and then were irradiated for 60 min in a ventilated Rayonet Photochemical Reactor under aerobic conditions.
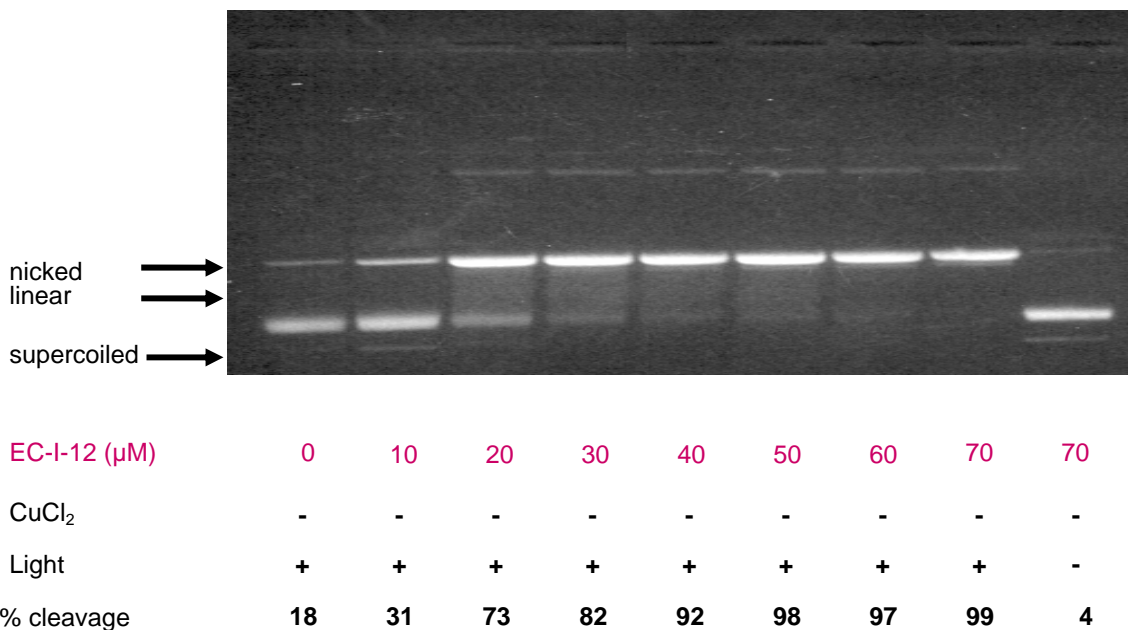

MP-I-73 (µM)	0	0	20	30	40	50	60	70	80	80
$CuCl_2$	+	+	+	+	+	+	+	+	+	-
Light	-	+	+	+	+	+	+	+	+	+
% cleavage	10	16	59	69	84	93	94	99	100	46

Figure 27 Concentration Titration, MP-I-73 with w/CuCl₂. Minimum concentration of compound **6** required for ≥ 90% conversion of supercoiled pUC19 plasmid to nicked/linear forms in the presence of equimolar copper(II). Samples were irradiated with eight 419 nm lamps. Each of the samples was prepared in the presence of 20 mM sodium phosphate buffer pH 7.0 and 38.5 µM bp pUC19 DNA, in a 20 µL reaction volume. The samples were allowed to preequilibrate at room temperature for 60 min and then were irradiated for 60 min in a ventilated Rayonet Photochemical Reactor under aerobic conditions with eight 419 nm lamps.
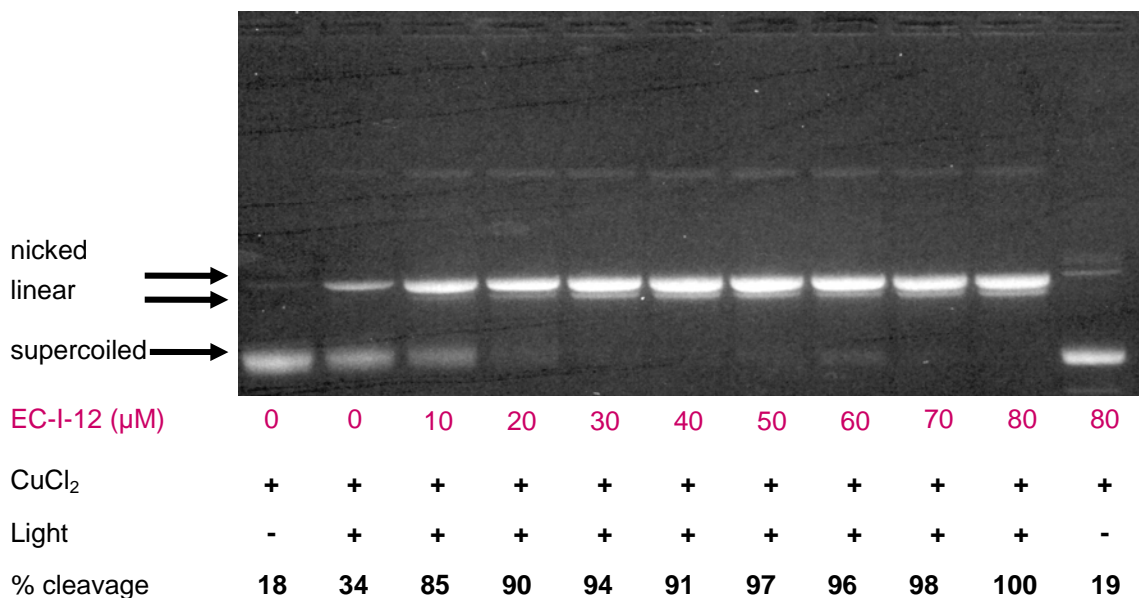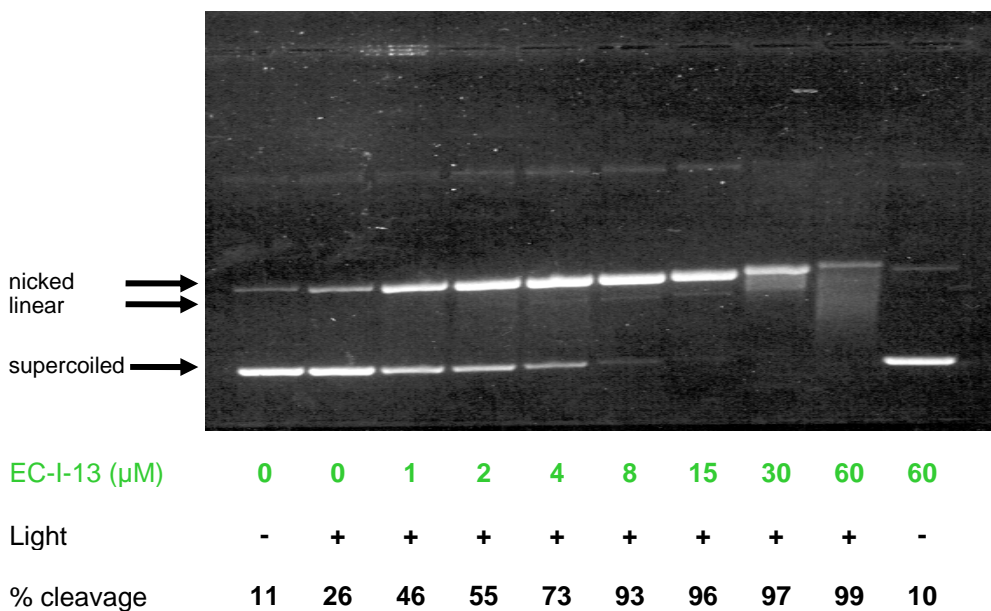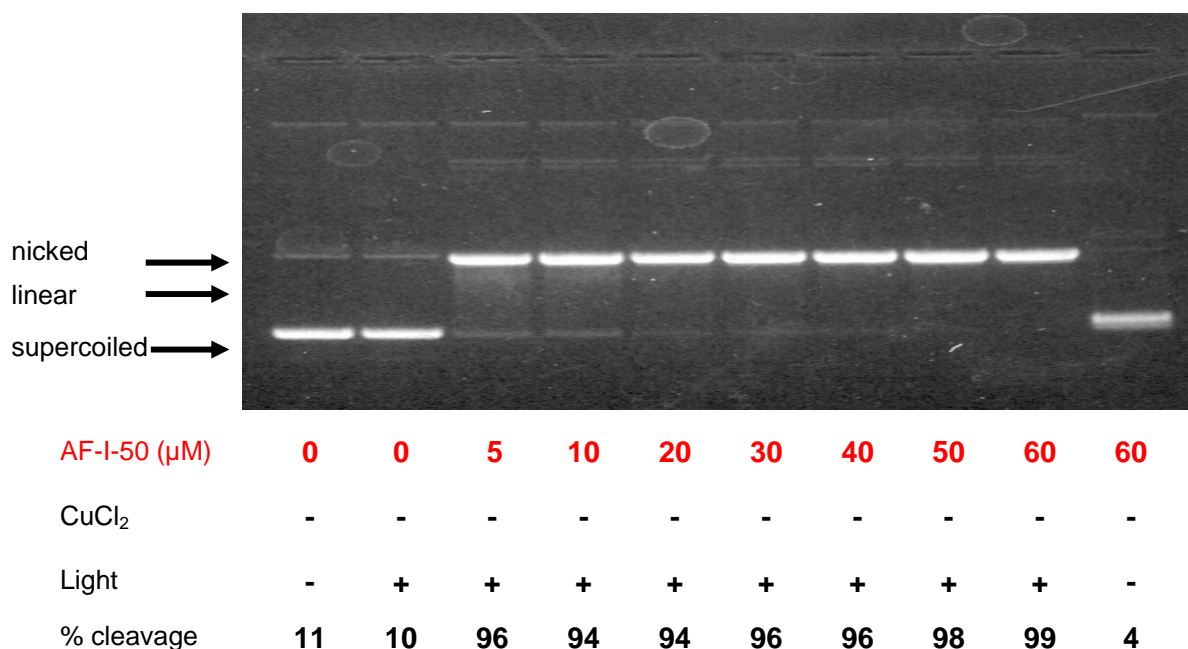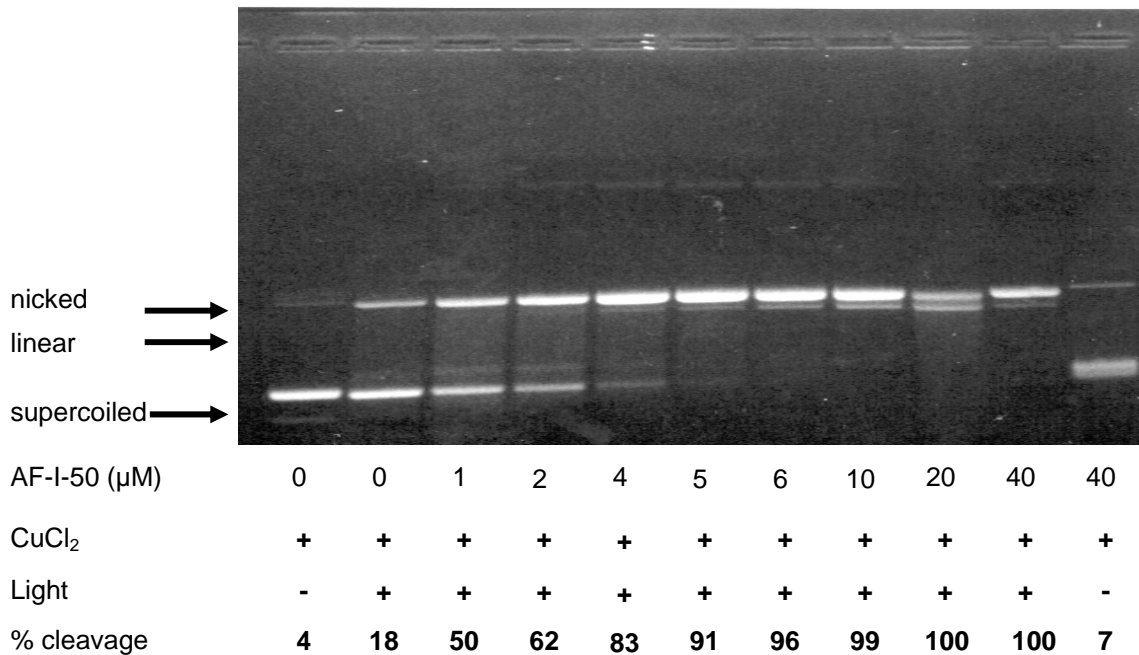
In this series of experiments, the minimal concentration required for a 90% or greater conversion of supercoiled DNA to nicked or linear forms was identified for each of the compounds under investigation. In each case, the concentrations were in the micromolar range. Compounds **3**, **5** and **6** were also found to exhibit enhanced performance in the presence of 1:1 equivalents of copper(II). This is promising considering the importance of copper(II) and its distribution in biological systems.[49, 50] From the values obtain in these experiments, the compounds can be ranked in order of increasing photocleavage effiencies as follows: **2 > 1 ≈ 5 > 4 > 3 > 6**. This ordering remains the same in the presence and absence of copper(II), with the exception of compound **5** which, when in the presence of Cu(II), cleaves DNA more efficiently than compound **1**. Interestingly, the ordering of T_m values in the absence of Cu(II) is: **2 > 4 > 5 > 6 > 3**. (The T_m value for **1** could not be determined due to decomposition of the compound.) Thus, for the majority of the compounds, the general trend is that photocleavage efficiency increases as a function of increasing T_m, which may reflect increasing binding affinity of the compounds to DNA.

Photocleavage of pUC19 dsDNA, Time Course Experiments

Concentrations similar to those which were used to achieve ≥ 90% DNA cleavage during 60 min of irradiation were used to investigate cleavage kinetics. In this series of experiments, individual reactions were prepared and irradiated in 10 min increments. The reaction products were then resolved on 1.0 % agarose gels (Figures 28 to 36). Gel images were captured with a Polaroid Gelcam and then quantified with a Molecular Dynamics FluorImager SI Gel Imaging System (Molecular Dynamics). Background corrections were done through a local averaging method.
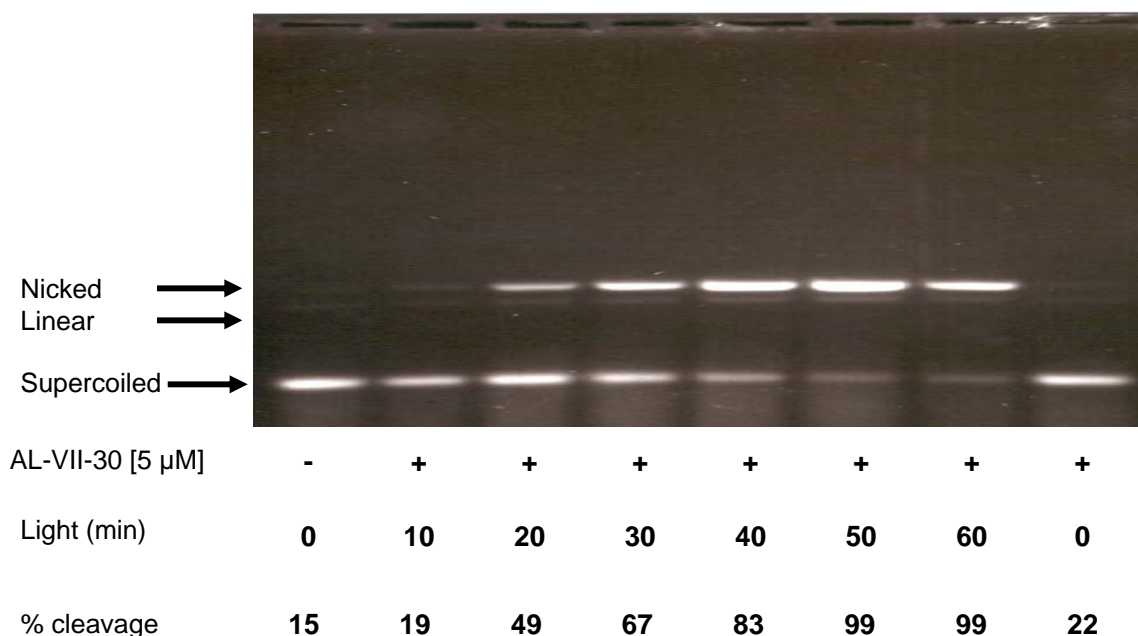
Figure 28 Time Course Experiment, AL-VII-30, Compound 1. Each of the samples was prepared in the presence of 5 µM compound, 20 mM sodium phosphate buffer pH 7.0 and 38.5 µM bp pUC19 DNA, in a 20 µL reaction volume. The samples were allowed to preequilibrate at room temperature for 60 min and then were irradiated at room temperature in a ventilated Rayonet Photochemical Reactor under aerobic conditions with eleven 350 nm lamps for time periods from 0-60 min.
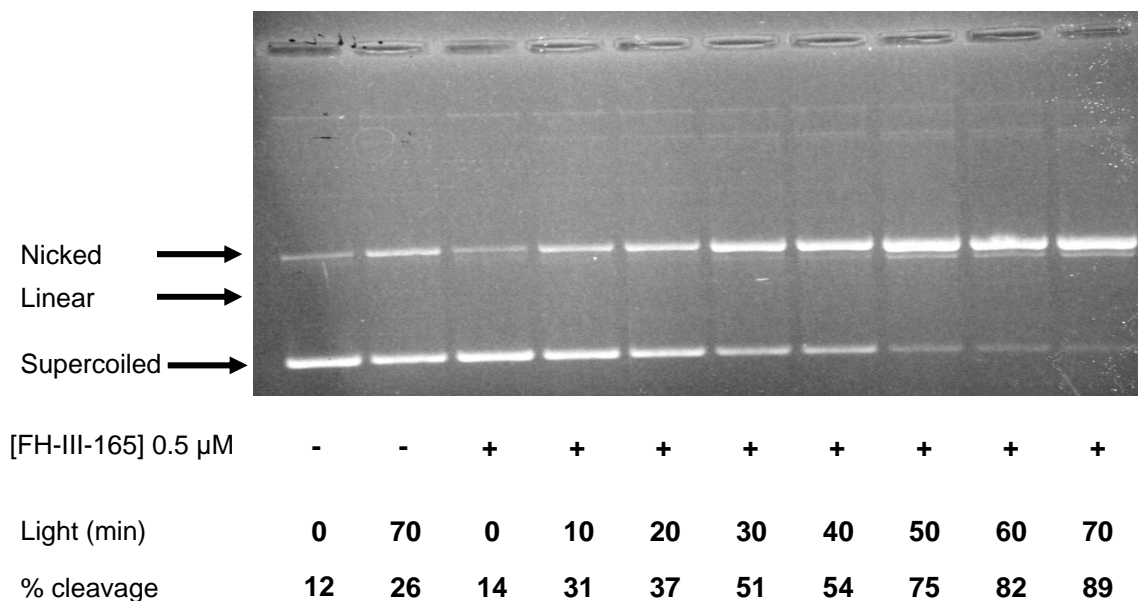
Figure 29 Time Course Experiment, AL-VII-30, Compound 2. Each of the samples was prepared in the presence of 0.5 µM compound, 20 mM sodium phosphate buffer pH 7.0 and 38.5 µM bp pUC19 DNA, in a 20 µL reaction volume. The samples were allowed to preequilibrate at room temperature for 60 min and then were irradiated at room temperature in a ventilated Rayonet Photochemical Reactor under aerobic conditions with eleven 350 nm lamps for time periods from 0-70 min.
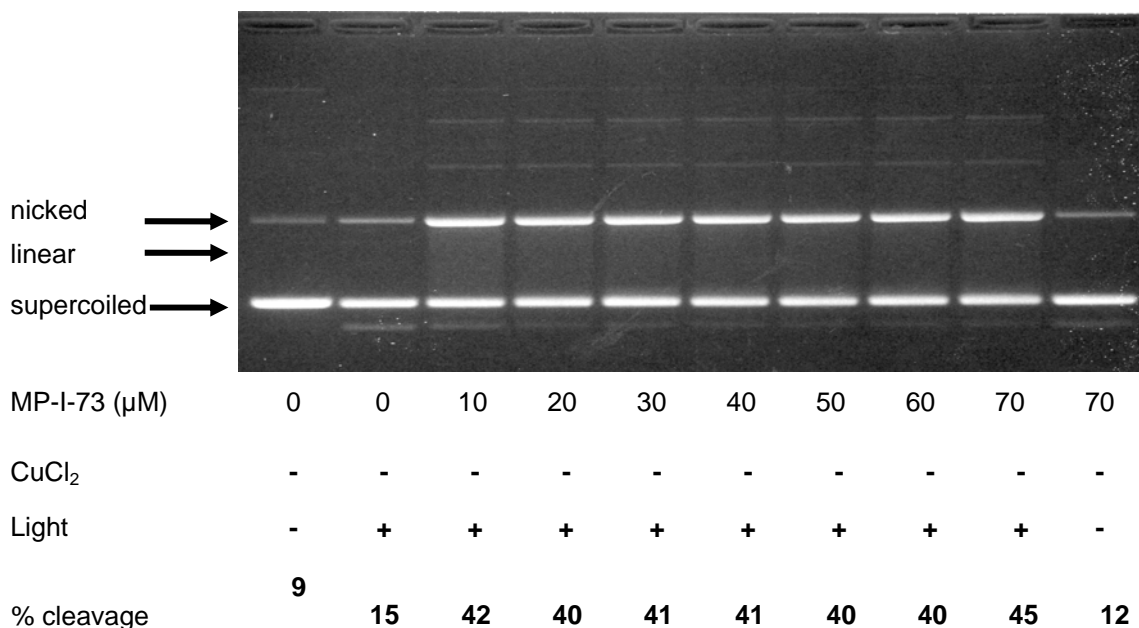
EC-I-12 [20 µM]	-	+	+	+	+	+	+	+	+
Light (min)	0	0	0	10	20	30	40	50	60
CuCl₂	-	-	-	-	-	-	-	-	-
% cleavage	12	12	18	29	37	42	46	51	55

Figure 30 Time Course Experiment, EC-I-12 w/o Cu(II), Compound 3 Each of the samples was prepared in the presence of 20 µM compound, 20 mM sodium phosphate buffer pH 7.0 and 38.5 µM bp pUC19 DNA, in a 20 µL reaction volume. The samples were allowed to preequilibrate at room temperature for 60 min and then were irradiated at room temperature in a ventilated Rayonet Photochemical Reactor under aerobic conditions with eleven 350 nm lamps for time periods from 0-60 min.
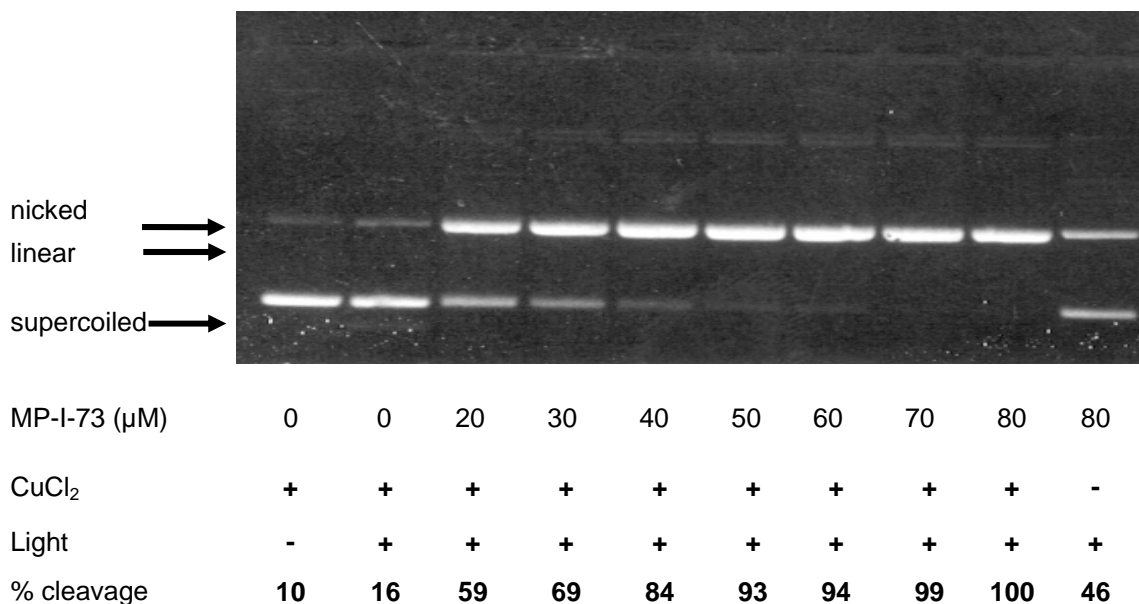

EC-I-12 [20 µM]	-	-	+	+	+	+	+	+	+	+
Light (min)	0	70	0	10	20	30	40	50	60	70
CuCl₂	+	+	+	+	+	+	+	+	+	+
% cleavage	11	39	24	51	64	78	85	95	94	98

Figure 31 Time Course Experiment, EC-I-12, Compound 3 Each of the samples was prepared in the presence of 20 µM compound, and equimolar CuCl₂, 20 mM sodium phosphate buffer pH 7.0 and 38.5 µM bp pUC19 DNA, in a 20 µL reaction volume. The samples were allowed to preequilibrate at room temperature for 60 min and then were irradiated at room temperature in a ventilated Rayonet Photochemical Reactor under aerobic conditions with eleven 350 nm lamps for time periods from 0-70 min.

EC-I-13 [10 µM]	-	-	+	+	+	+	+	+	+	+
Light (min)	0	70	0	10	20	30	40	50	60	70
% cleavage	12	23	4	44	66	78	90	93	99	99

Figure 32 Time Course Experiment, EC-I-13, Compound 4 Each of the samples was prepared in the presence of 10 µM compound, 20 mM sodium phosphate buffer pH 7.0 and 38.5 µM bp pUC19 DNA, in a 20 µL reaction volume. The samples were allowed to preequilibrate at room temperature for 60 min and then were irradiated at room temperature in a ventilated Rayonet Photochemical Reactor under aerobic conditions with eleven 350 nm lamps for time periods from 0-70 min.

|								
[AF-I-50] µM	-	-	+	+	+	+	+	+	+
Light (min)	0	50	0	10	20	30	40	50	60
$CuCl_2$	-	-	-	-	-	-	-	-	-
% cleavage	87	10	11	79	92	95	96	98	99

Figure 33 Time Course Experiment, AF-I-50, Compound 5. Each of the samples was prepared in the presence of 5 µM compound, 20 mM sodium phosphate buffer pH 7.0 and 38.5 µM bp pUC19 DNA, in a 20 µL reaction volume. The samples were allowed to preequilibrate at room temperature for 60 min and then were irradiated at room temperature in a ventilated Rayonet Photochemical Reactor under aerobic conditions with eight 419 nm lamps for time periods from 0-60 min.

[AF-I-50]	-	+	+	+	+	+	+	+	+	+
Light (min)	0	70	0	10	20	30	40	50	60	70
CuCl	+	+	+	+	+	+	+	+	+	+
% cleavage	8	9	6	95	100	100	99	95	100	100
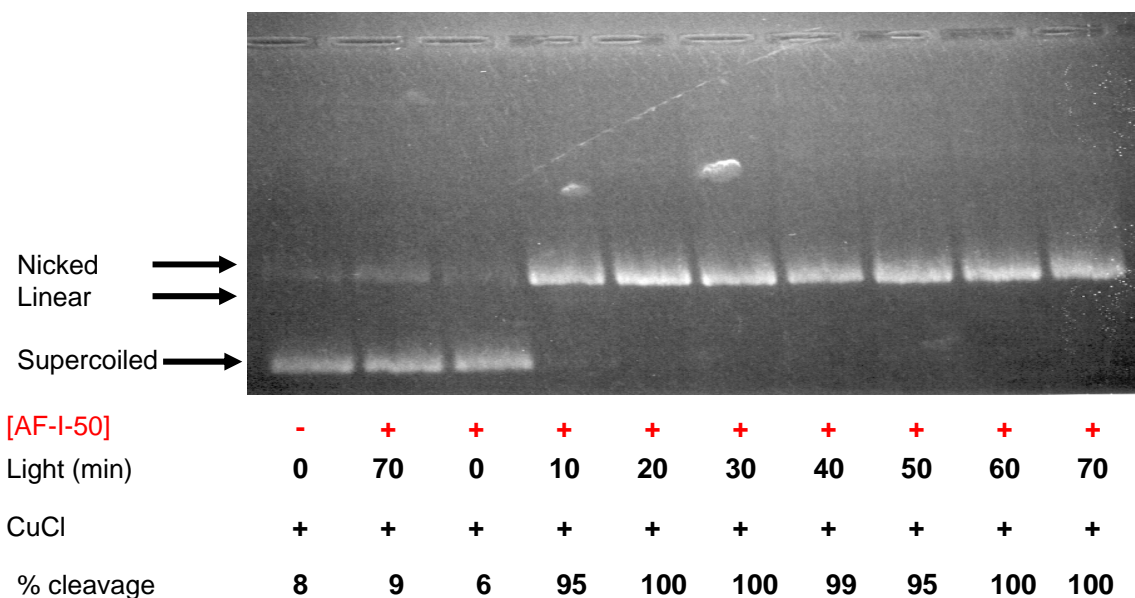
Figure 34 Time Course Experiment, AF-I-50 w/CuCl₂, Compound 5. Each of the samples was prepared in the presence of 5 µM compound, 20 mM sodium phosphate buffer pH 7.0 and 38.5 µM bp pUC19 DNA, and 5 µM CuCl₂ in a 20 µL reaction volume. The samples were allowed to preequilibrate at room temperature for 60 min and then were irradiated at room temperature in a ventilated Rayonet Photochemical Reactor under aerobic conditions with eight 419 nm lamps for time periods from 0-70 min.


[MP-I-73] 50 µM	-	-	+	+	+	+	+	+	+	+
Light (min)	0	70	0	10	20	30	40	50	60	70
CuCl₂	-	-	-	-	-	-	-	-	-	-
% cleavage	20	18	21	27	29	36	39	41	40	41
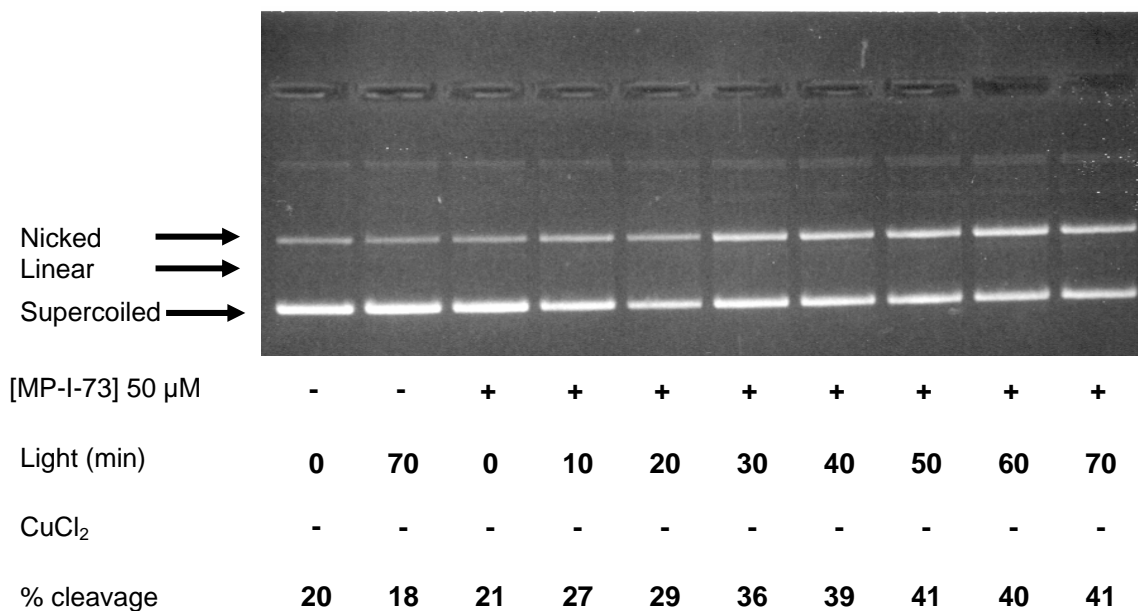
Figure 35 Time Course Experiment MP-I-73 w/o CuCl₂, Compound 6. Each of the samples was prepared in the presence of 50 µM compound, 20 mM sodium phosphate buffer pH 7.0 and 38.5 µM bp pUC19 DNA, in a 20 µL reaction volume. The samples were allowed to preequilibrate at room temperature for 60 min and then were irradiated at room temperature in a ventilated Rayonet Photochemical Reactor under aerobic conditions with eight 419 nm lamps for time periods from 0-70 min.
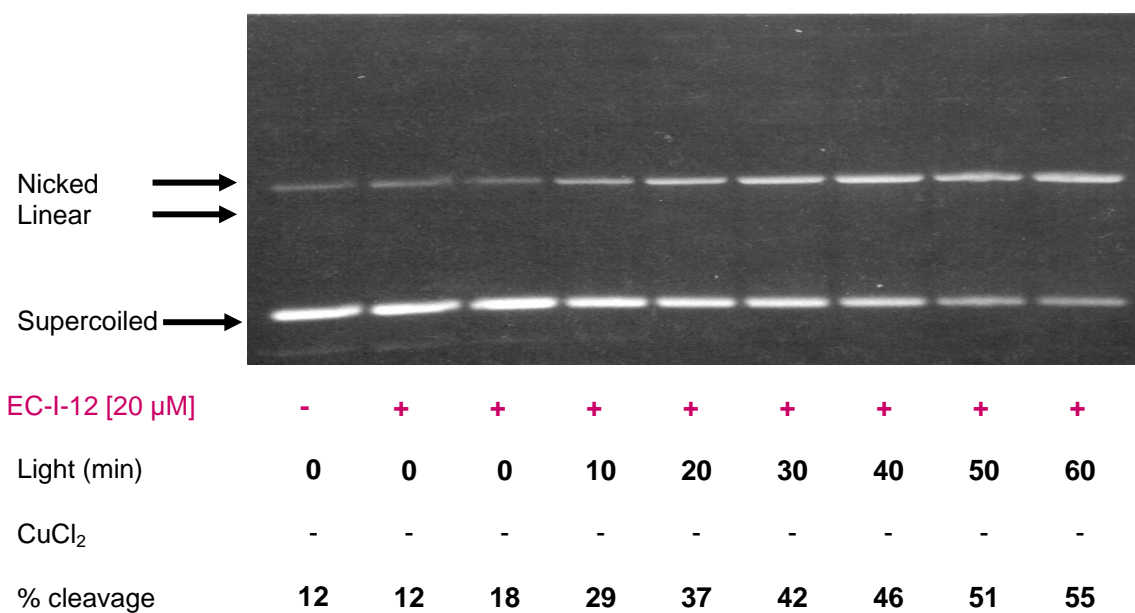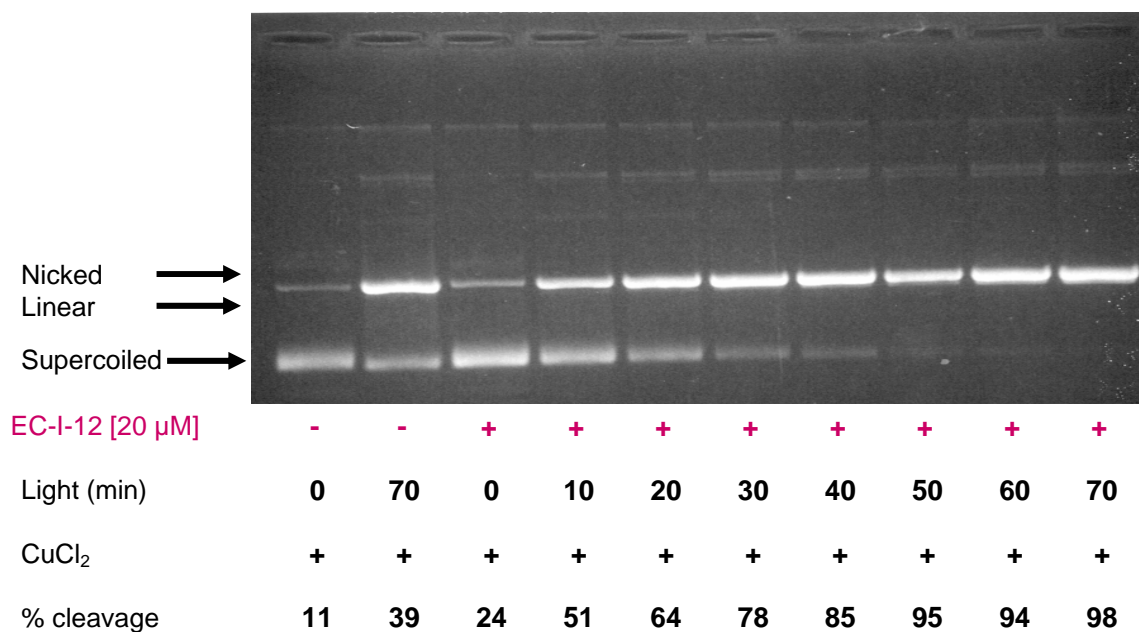
43

Nicked								
Linear								
Supercoiled								
[MP-I-73] 50 µM	-	-	+	+	+	+	+	+	+
Light (min)	0	0	10	20	30	40	50	60	70
CuCl$_2$	+	+	+	+	+	+	+	+	+
% cleavage	30	34	42	55	65	76	86	90	92
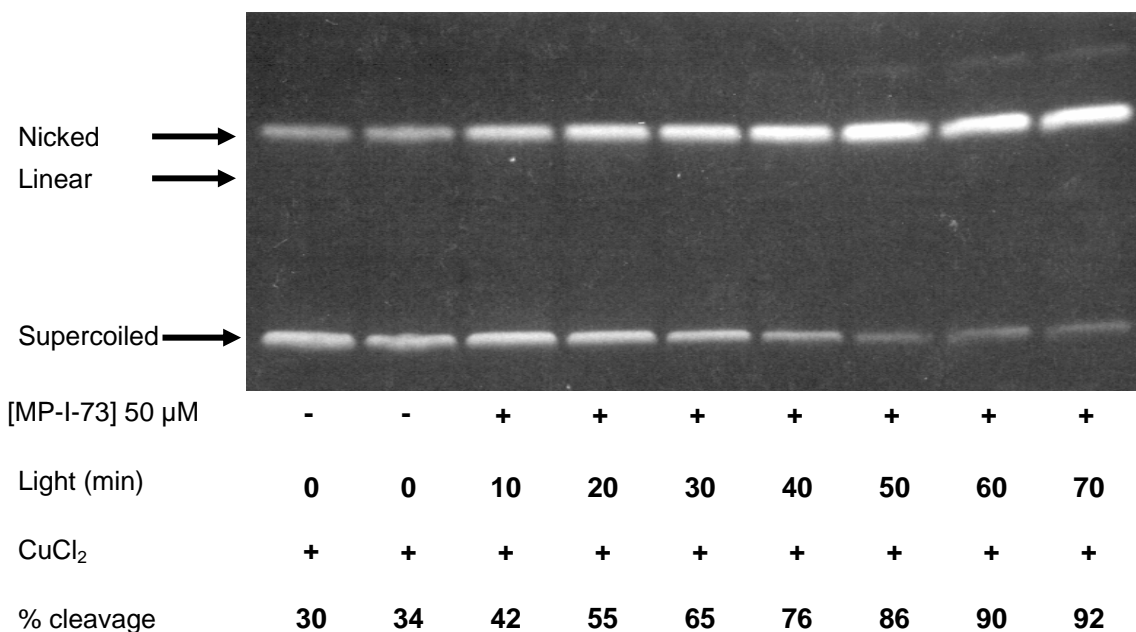
Figure 36 Time Course Experiment MP-I-73 w/ Cu (II), Compound 6. Each of the samples was prepared in the presence of 50 µM compound and 1:1 equiv CuCl$_2$, 20 mM sodium phosphate buffer pH 7.0 and 38.5 µM bp pUC19 DNA, in a 20 µL reaction volume. The samples were allowed to preequilibrate at room temperature for 60 min and then were irradiated at room temperature in a ventilated Rayonet Photochemical Reactor under aerobic conditions with eight 419 nm lamps for time periods from 0-70 min.
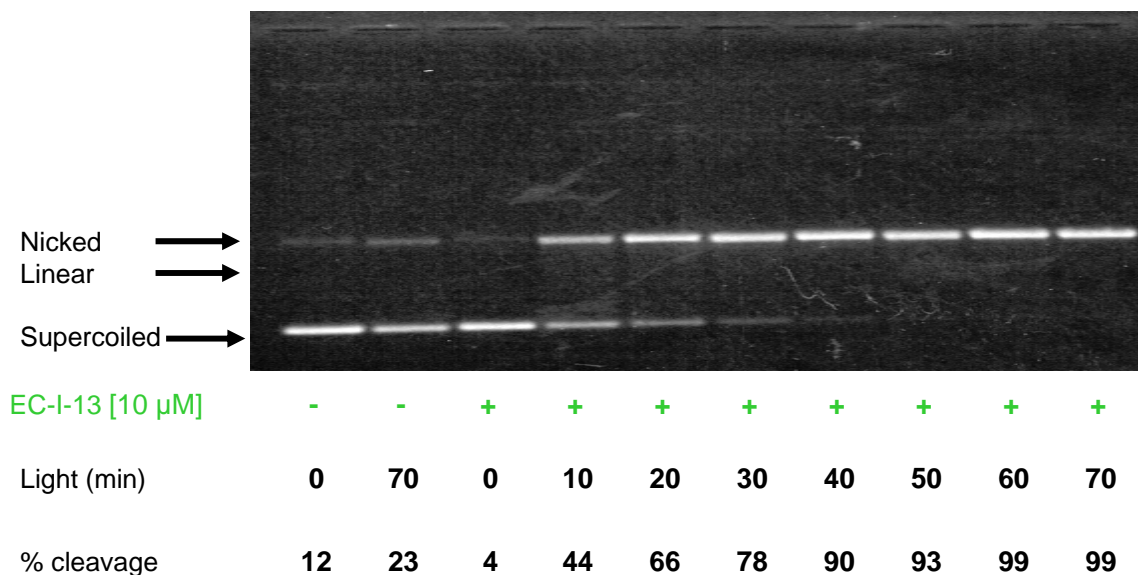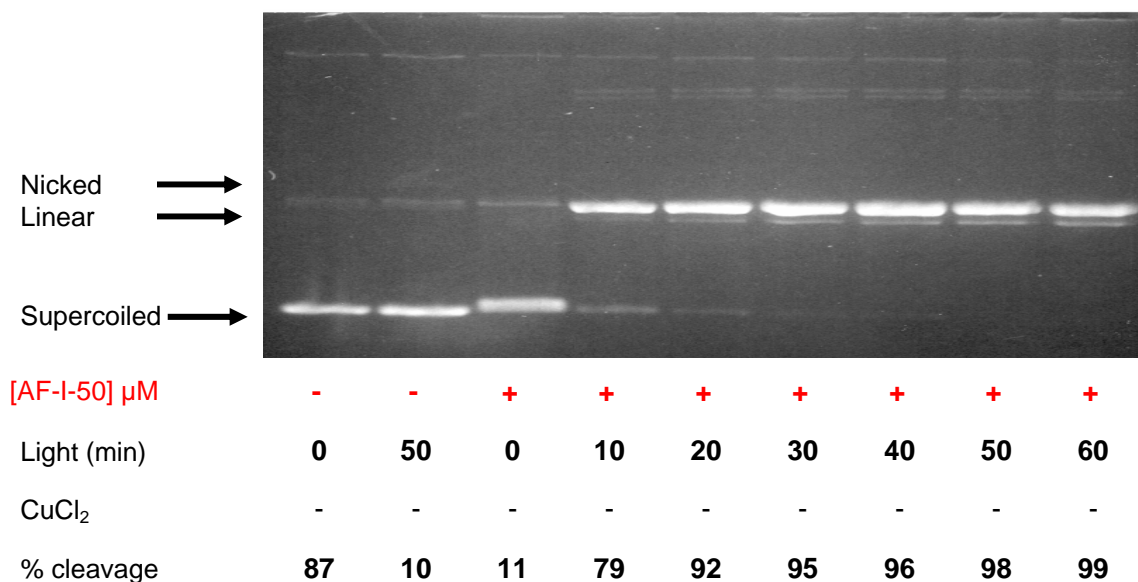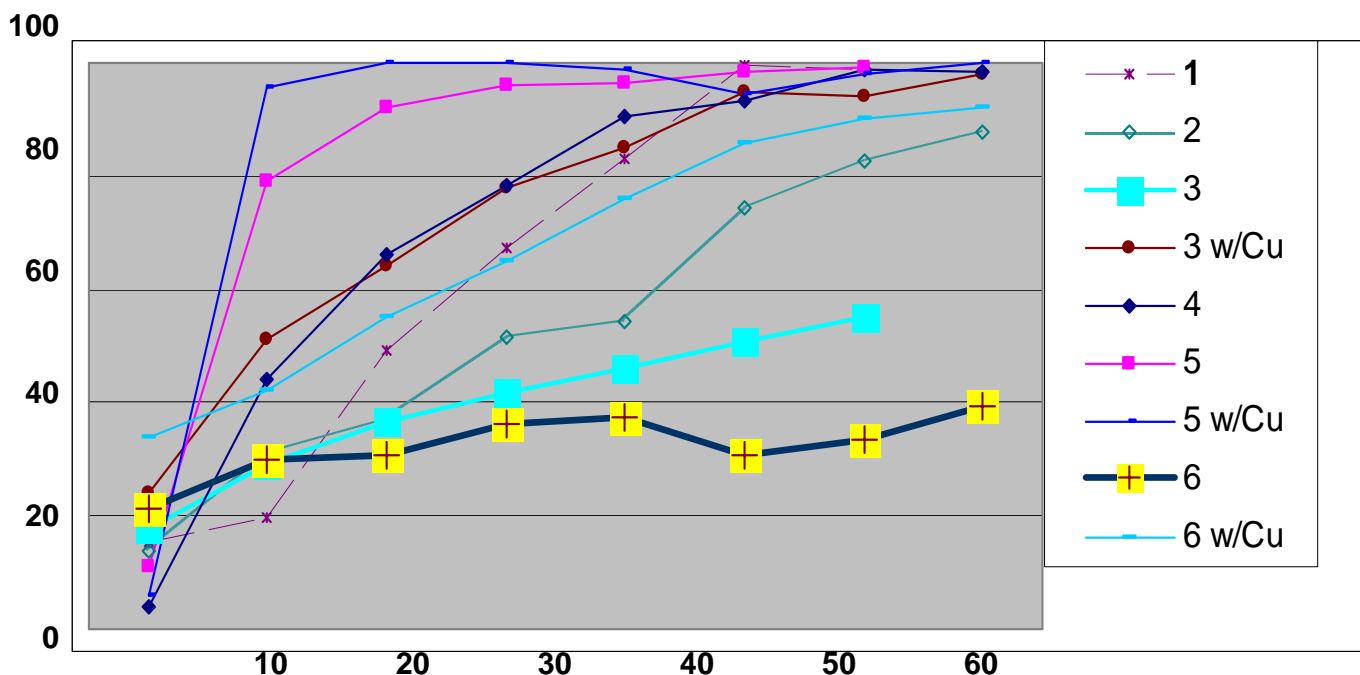

Figure 37 Time Course Experiments. Time dependent analysis of the progression of photocleavage. Samples were prepared using the following concentrations of compound: Compound **1**, 5 µM; Compound **2**, 0.5 µM; Compound **3**, 20 µM; Compound **4**, 10 µM; Compound **5**, 5 µM; Compound **6**, 50 µM. Each of the samples was prepared in the presence of 20 mM sodium phosphate buffer pH 7.0 and 38.5 µM bp pUC19 DNA, in a 20 µL reaction volume. The samples were allowed to preequilibrate at room temperature for 60 min and then were irradiated at room temperature for 0-60 min in a ventilated Rayonet Photochemical Reactor under aerobic conditions. Compounds **1**, **2**, **3**, and **4** were irradiated with eleven 350 nm lamps, while **5** and **6** were irradiated with eight 419 nm lamps.

This series of experiments was employed to examine DNA photocleavage kinetics. From the data gathered at t = 10 min (Figure 37), the compounds can be ranked in order of decreasing rate as follows: **5** w/Cu > **5** w/o Cu > **3** w/ Cu > **4** > **6** w/Cu > **2** > **3** w/o Cu > **6** w/o Cu > **1**.

Photocleavage of pUC19 dsDNA, Radical Scavenger Assay

To investigate the mechanism(s) involved in DNA photocleavage, we conducted inhibition experiments in which DNA photocleavage reactions were conducted in the presence of several scavengers: sodium azide for $^1O_2$, catalase for H_2O_2, superoxide dismutase (SOD) for $O_2^{\cdot-}$, D-mannitol, D-sorbitol, and sodium benzoate for $\cdot OH$ (Figures 38 to 43). If the scavenger is successful in inhibiting DNA damage, then this should correspond to an increase in the amount of supercoiled DNA and a corresponding decrease in the quantity of the nicked and linear forms. A summary of the data obtained from these studies is in Table 5.

The results of this investigation strongly suggests that the photocleavage of DNA occurs as a result of a combinations of type I and type II mechanisms in the case of compounds **3**, **5** and **6**. From the information obtain in this series of experiments, there is a suggestion that singlet oxygen may be involved in DNA photocleavage by all six investigational compounds due to the decrease in cleavage seen in the presence of the singlet oxygen scavenger sodium azide (Table 5). For the planar phenazine compound **3,** there was also a significant inhibition in cleavage yields observed in the presence of the superoxide scavenger superoxide dismutase, as well as in the presence of the hydroxyl radical scavenger sodium benzoate. Compound **5** also exhibits reduced photocleavage in

the presence of the hydroxyl radical scavenger, sodium benzoate. Alternatively,

photocleavage by compound **6** is strongly inhibited by the H_2O_2 scavenger catalase.

AL-VII-30 5 µM	-	-	+	+	+	+	+	+	+	+	+
Scavenger	-	-	-	1	2	3	4	5	6	7	-
Light	-	+	+	+	+	+	+	+	+	+	-

Figure 38 Scavenger Assay AL-VII-30, Compound 1. Percent inhibition of DNA photocleavage in the presence of scavengers. Each of the samples was prepared in the presence of 20 mM sodium phosphate buffer pH 7.0 and 38.5 µM bp pUC19 DNA, in a 20 µL reaction volume. The following concentrations of scavengers were added: Na Azide - 100 mM, catalase - 50 Units, SOD - 50 Units, catalase + SOD - 50 Units each, D-mannitol - 20 mM, D-sorbitol - 20 mM, Na Benzoate - 100 mM. Then, samples were allowed to preequilibrate at room temperature for 60 min and were irradiated for 50 min in a ventilated Rayonet Photochemical Reactor under aerobic condition.

FH-III-165 (0.5 µM)	-	-	+	+	+	+	+	+	+	+	+
Scavenger	-	-	-	1	2	3	4	5	6	7	-
Light	-	+	+	+	+	+	+	+	+	+	-
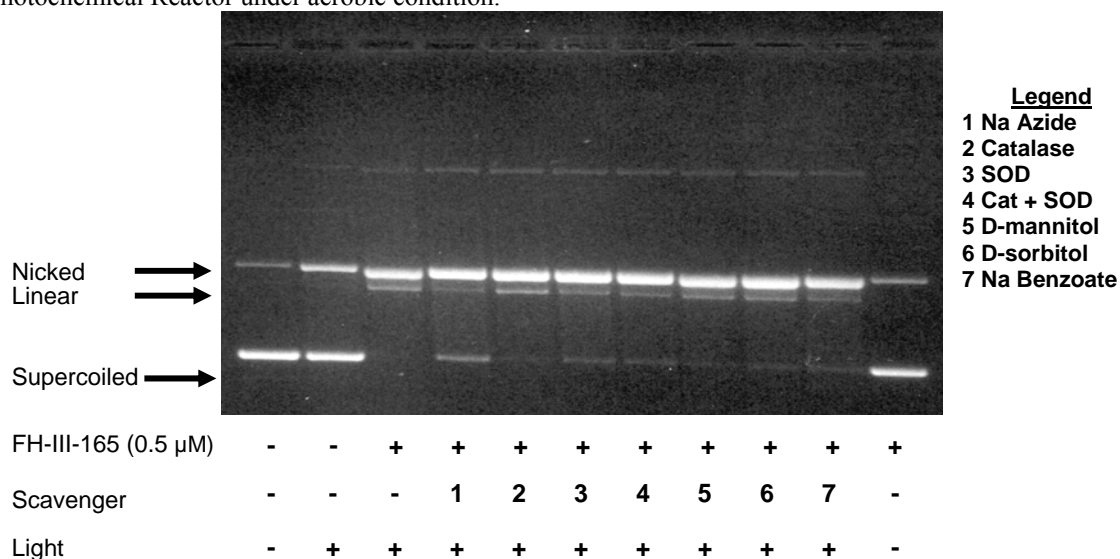
Figure 39 Scavenger Assay FH-III-165, Compound 2. Percent inhibition of DNA photocleavage in the presence of scavengers. Each of the samples was prepared in the presence of 20 mM sodium phosphate buffer pH 7.0 and 38.5 µM bp pUC19 DNA, in a 20 µL reaction volume. The following concentrations of scavengers were added: Na Azide - 100 mM, catalase - 50 Units, SOD - 50 Units, catalase + SOD - 50 Units each, D-mannitol - 20 mM, D-sorbitol - 20 mM, Na Benzoate - 100 mM. Then, samples were allowed to preequilibrate at room temperature for 60 min and were irradiated for 50 min in a ventilated Rayonet Photochemical Reactor under aerobic condition.

Figure 40 Scavenger Assay EC-I-12, Compound 3. Percent inhibition of DNA photocleavage in the presence of scavengers. Each of the samples was prepared in the presence of 20 mM sodium phosphate buffer pH 7.0, 20 µM compound **3**, equimolar copper chloride, and 38.5 µM bp pUC19 DNA, in a 20 µL reaction volume. The following concentrations of scavengers were added: Na Azide - 100 mM, catalase - 50 Units, SOD - 50 Units, catalase + SOD - 50 Units each, D-mannitol - 20 mM, D-sorbitol - 20 mM, Na Benzoate - 100 mM. Then, samples were allowed to preequilibrate at room temperature for 60 min and were irradiated for 50 min in a ventilated Rayonet Photochemical Reactor under aerobic condition.
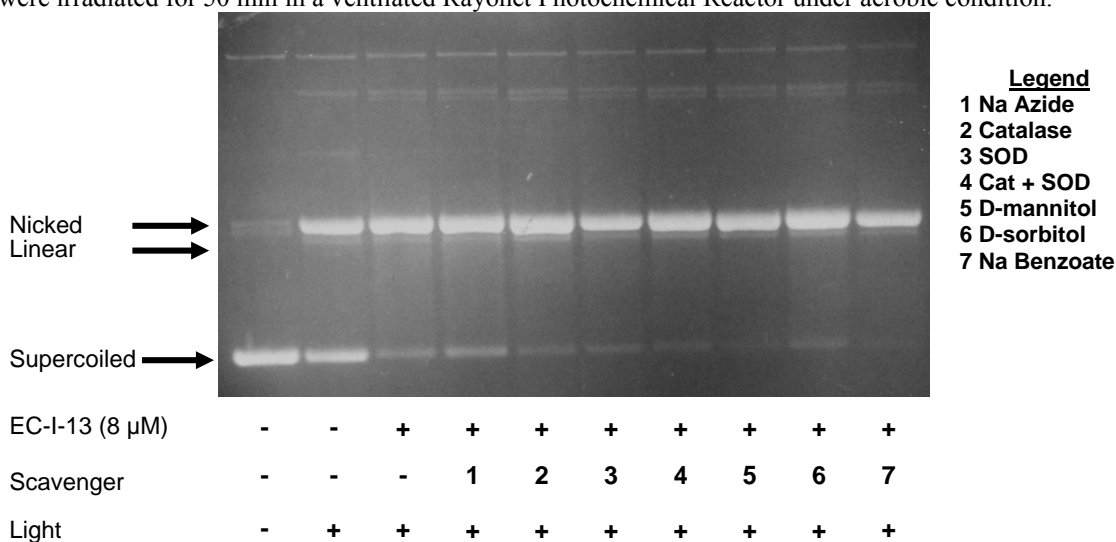
Figure 41 Scavenger Assay EC-I-13, Compound 4. Percent inhibition of DNA photocleavage in the presence of scavengers. Each of the samples was prepared in the presence of 20 mM sodium phosphate buffer pH 7.0 and 38.5 µM bp pUC19 DNA, in a 20 µL reaction volume. The following concentrations of scavengers were added: Na Azide - 100 mM, catalase - 50 Units, SOD - 50 Units, catalase + SOD - 50 Units each, D-mannitol - 20 mM, D-sorbitol - 20 mM, Na Benzoate - 100 mM. Then, samples were allowed to preequilibrate at room temperature for 60 min and were irradiated for 50 min in a ventilated Rayonet Photochemical Reactor under aerobic condition.

Nicked
Linear

Supercoiled

AF-I-50 [5 µM]	-	-	+	+	+	+	+	+	+	+	+
Scavenger	-	-	-	-	1	2	3	4	5	6	7
Light	-	+	-	+	+	+	+	+	+	+	+

Legend
1 Na Azide
2 Catalase
3 SOD
4 cat + SOD
5 D-mannitol
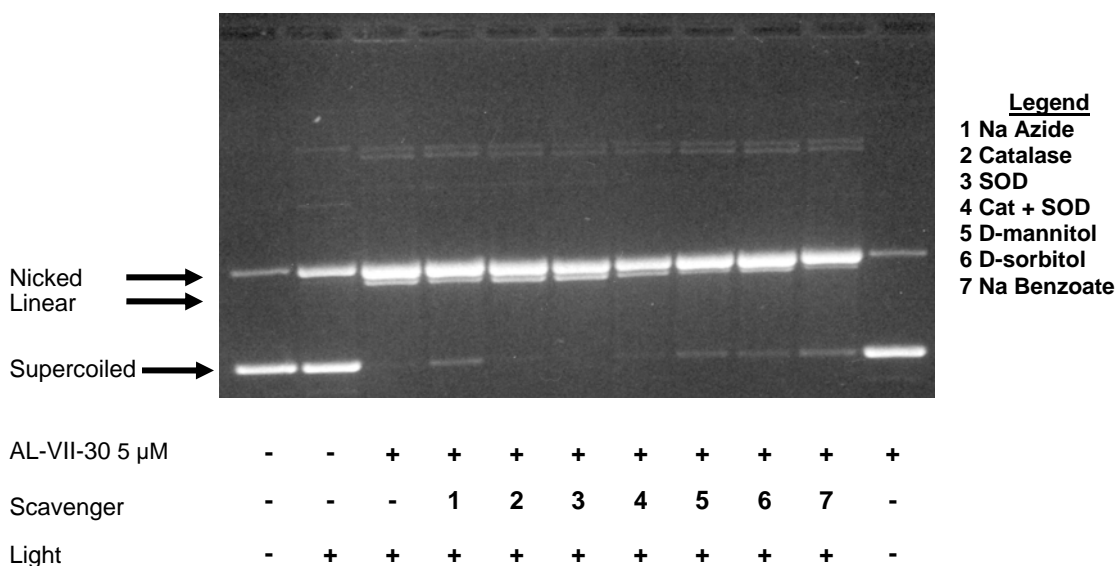**6 D-sorbitol**
7 Na Benzoate

Figure 42 Scavenger Assay AF-I-50, Compound 5. Percent inhibition of DNA photocleavage in the presence of scavengers. Each of the samples was prepared in the presence of 20 mM sodium phosphate buffer pH 7.0 and 38.5 µM bp pUC19 DNA, in a 20 µL reaction volume. The following concentrations of scavengers were added: Na Azide - 100 mM, catalase - 50 Units, SOD - 50 Units, catalase + SOD - 50 Units each, D-mannitol - 20 mM, D-sorbitol - 20 mM, Na Benzoate - 100 mM. Then, samples were allowed to preequilibrate at room temperature for 60 min and were irradiated for 50 min in a ventilated Rayonet Photochemical Reactor under aerobic condition.


Nicked
Linear
Supercoiled

MP-I-73 [50 µM]	-	-	+	+	+	+	+	+	+	+	+
Scavenger	-	-	-	1	2	3	4	5	6	7	-
CuCl₂	+	+	+	+	+	+	+	+	+	+	+
Light	-	+	+	+	+	+	+	+	+	+	-

Legend
1 Na Azide
2 Catalase
3 SOD
4 Cat + SOD
5 D-mannitol
6 D-sorbitol
7 Na Benzoate

Figure 43 Scavenger Assay MP-I-73, Compound 6. Percent inhibition of DNA photocleavage in the presence of scavengers. Each of the samples was prepared in the presence of equimolar copper chloride, 20 mM sodium phosphate buffer pH 7.0 and 38.5 µM bp pUC19 DNA, in a 20 µL reaction volume. The following concentrations of scavengers were added: Na Azide - 100 mM, catalase - 50 Units, SOD - 50 Units, catalase + SOD - 50 Units each, D-mannitol - 20 mM, D-sorbitol - 20 mM, Na Benzoate - 100 mM. Then, samples were allowed to preequilibrate at room temperature for 60 min and were irradiated for 50 min in a ventilated Rayonet Photochemical Reactor under aerobic condition.
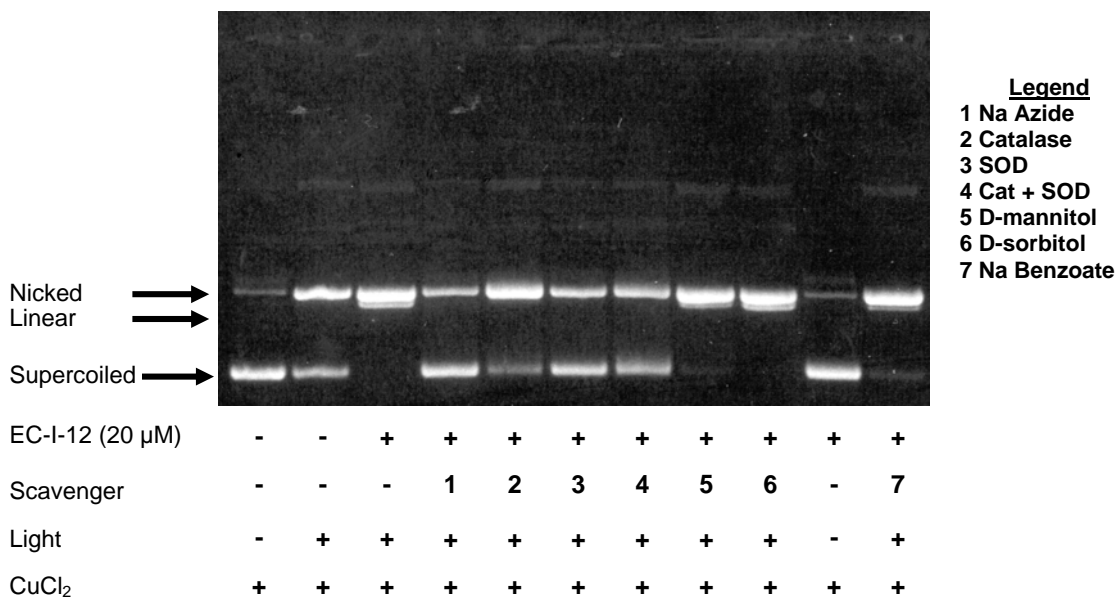
Compound	% Cleavage	% Inhibition with Scavenger						
		Na Azide ($^1O_2$)	Catalase (H_2O_2)	SOD ($O_2^{\cdot-}$)	Catalase + SOD	D-mannitol (•OH)	D-sorbitol (•OH)	Na Benzoate (•OH)
1	94 %	31%	3%	0%	0%	3%	4%	21%
2	99 %	36%	6%	14%	9%	0%	6%	9%
3	98 %	67%	24%	53%	44%	4%	0%	88%
4	95 %	35%	1%	3%	2%	3%	5%	1%
5	97 %	12%	1%	2%	3%	1%	1%	27%
6	95 %	30%	93%	12%	86%	7%	5%	0%

Table 5 Scavenger Assays. Percent inhibition of DNA photocleavage in the presence of scavenger.
Each of the samples was prepared in the presence of 20 mM sodium phosphate buffer pH 7.0 and 38.5 μM bp pUC19 DNA, in a 20 μL reaction volume. Next, the following concentrations of scavengers were added: Na Azide - 100 mM, catalase - 50 Units, SOD - 50 Units, catalase + SOD - 50 Units each, D-mannitol - 20 mM, D-sorbitol - 20 mM, Na Benzoate - 100 mM, and the samples were allowed to preequilibrate at room temperature for 60 min and then were irradiated for 50 min in a ventilated Rayonet Photochemi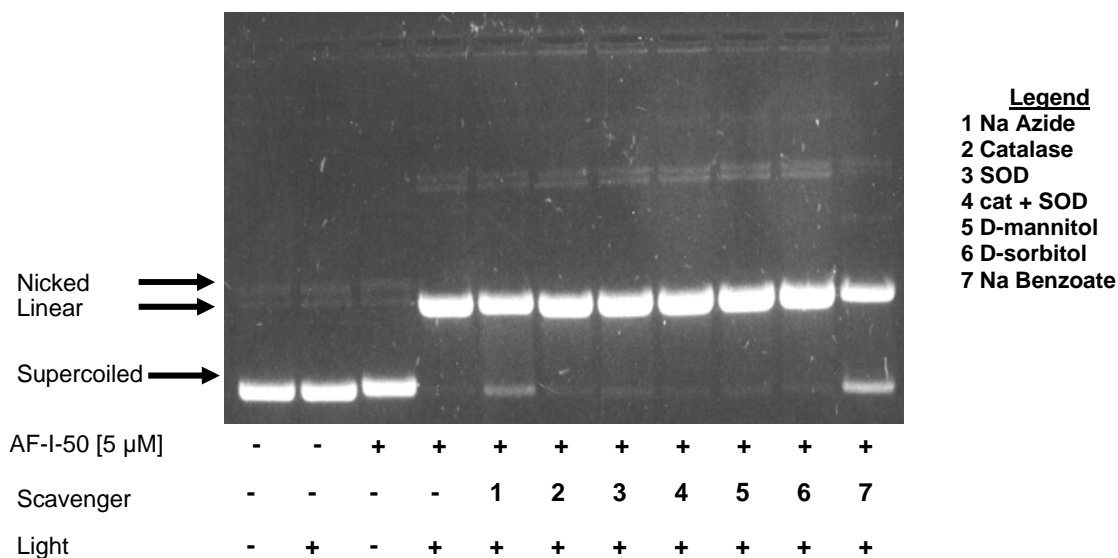cal Reactor under aerobic conditions. Compounds **2** and **6** were evaluated in the presence of equimolar concentrations of CuCl₂.

Photocleavage of pUC19 dsDNA, Salt Inhibition Assay

The investigational compounds contain positive charges at physiological pH,

which many assist in binding the compounds to the negatively charged DNA backbone.

In order to investigate the effect of competitive ions on the ability of these compound to

induce DNA damage, a series of assays was conducted in which increasing

concentrations of sodium chloride were titrated into the DNA photocleavage reactions

(Figures 44 to 52).

[AL-VII-30] 5 µM	-	+	+	+	+	+	+	+	+
[NaCl] mM	-	0	25	50	75	100	125	150	150
Light	+	+	+	+	+	+	+	+	-
% cleavage	10	98	25	26	28	27	31	26	11

Figure 44 Salt Challenge AL-VII-30, Compound 1. Each of the samples was prepared in the presence of 20 mM sodium phosphate buffer pH 7.0 and 38.5 µM bp pUC19 DNA, and 0-150 mM NaCl in a 20 µL reaction volume. The samples were allowed to preequilibrate at room temperature for 60 min and then were irradiated for 60 min in a ventilated Rayonet Photochemical Reactor with eleven 350 nm lamps.
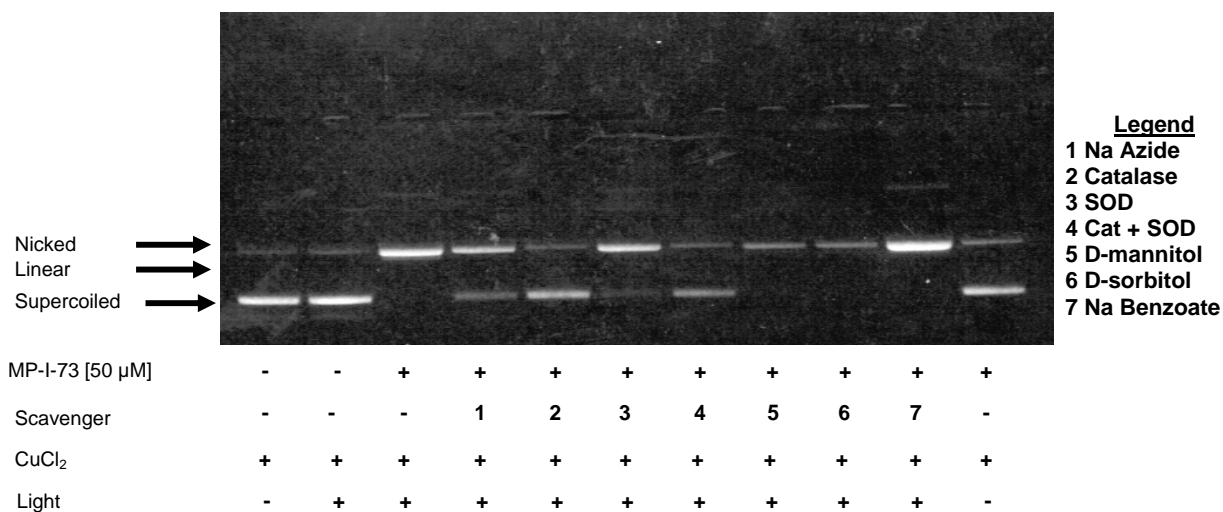

[FH-III-165] 0.5 µM	-	-	+	+	+	+	+	+	+	+
[NaCl] mM	-	-	0	25	50	75	100	125	150	150
Light	-	+	+	+	+	+	+	+	+	-
% cleavage	6	18	94	82	64	63	57	57	50	7

Figure 45 Salt Challenge FH-III-165, Compound 2. Each of the samples was prepared in the presence of 20 mM sodium phosphate buffer pH 7.0 and 38.5 µM bp pUC19 DNA, and 0-150 mM NaCl in a 20 µL reaction volume. The samples were allowed to preequilibrate at room temperature for 60 min and then were irradiated for 60 min at room temperature in a ventilated Rayonet Photochemical Reactor with eleven 350 nm lamps.

[EC-I-12] 20 µM	-	-	+	+	+	+	+	+	+	+
NaCl (mM)	-	-	0	25	50	75	100	125	150	150
CuCl$_2$	-	-	-	-	-	-	-	-	-	-
Light	-	+	+	+	+	+	+	+	+	+
% Cleavage	12	33	55	49	50	46	41	39	36	11

Figure 46 Salt Challenge EC-I-12 w/o Cu (II), Compound 3. Each of the samples was prepared in the presence of 20 mM sodium phosphate buffer pH 7.0 and 38.5 µM bp pUC19 DNA, 20 µM **3**, and 0-150 mM NaCl in a 20 µL reaction volume. The samples were allowed to preequilibrate at room temperature for 60 min and then were irradiated for 60 min at room temperature in a ventilated Rayonet Photochemical Reactor with eleven 350 nm lamps.

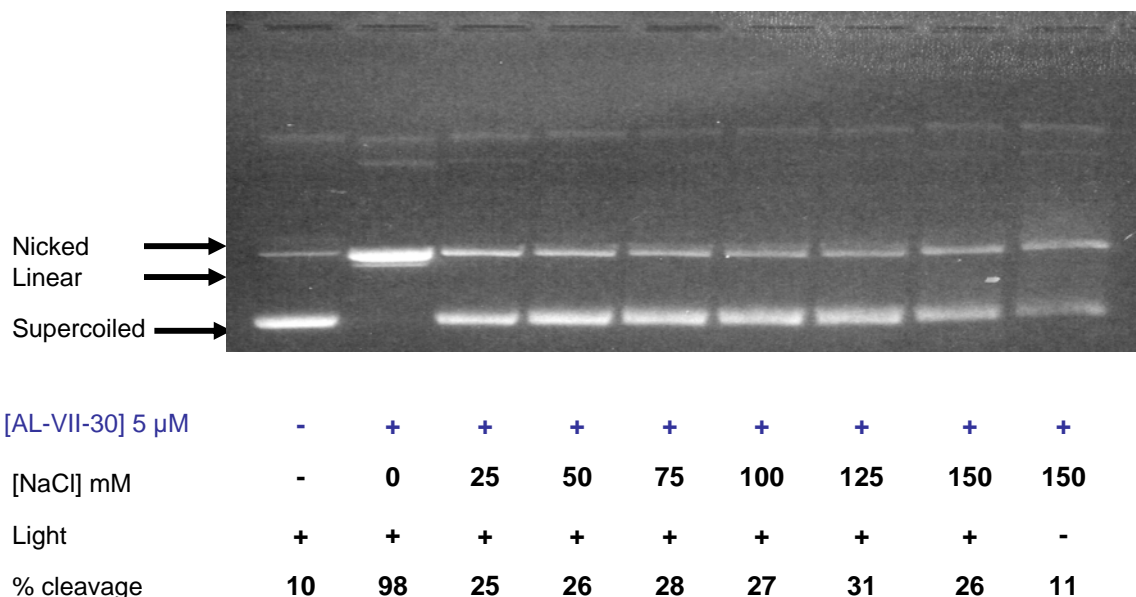| [EC-I-12] 20 µM	-	-	+	+	+	+	+	+	+	+
[NaCl] mM	-	-	0	25	50	75	100	125	150	150
Light	-	+	+	+	+	+	+	+	+	-
CuCl$_2$	+	+	+	+	+	+	+	+	+	+
% cleavage	11	27	95	87	88	82	80	78	81	10

Figure 47 Salt Challenge EC-I-12 w/ Cu (II), Compound 3. Each of the samples was prepared in the presence of 20 mM sodium phosphate buffer pH 7.0, equimolar copper chloride and 38.5 µM bp pUC19 DNA, 20 µM **3**, 1:1 of equiv CuCl$_2$, and 0-150 mM NaCl in a 20 µL reaction volume. The samples were allowed to preequilibrate at room temperature for 60 min and then were irradiated for 60 min at room temperature in a ventilated Rayonet Photochemical Reactor with eleven 350 nm lamps.

51

Nicked										
Linear										
Supercoiled										

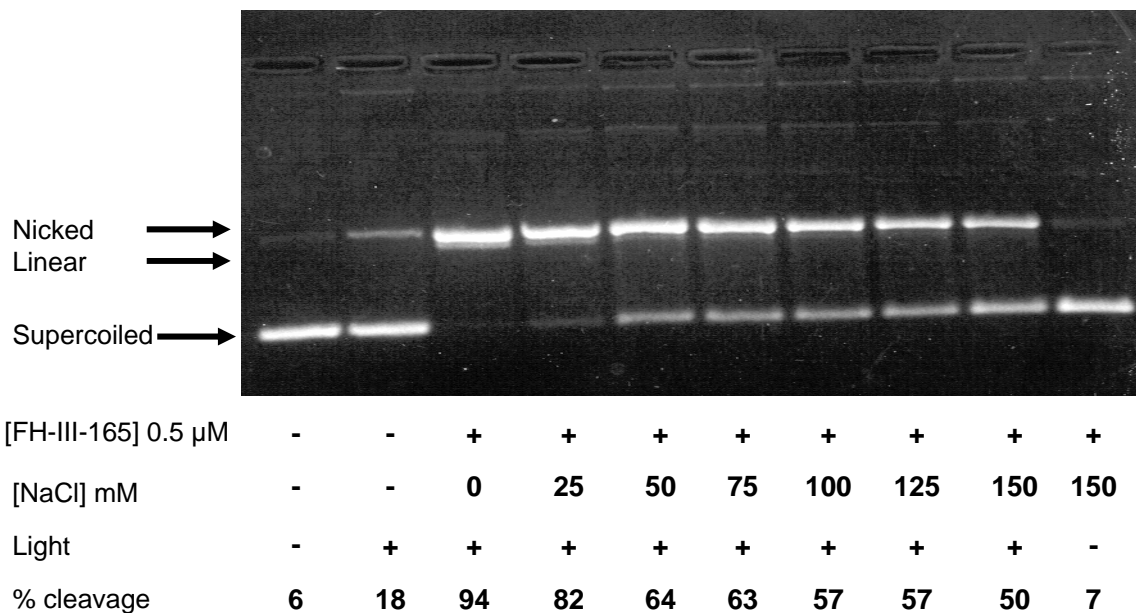| [EC-I-13] 10 µM	-	-	+	+	+	+	+	+	+	+
[NaCl] mM	-	-	0	25	50	75	100	125	150	150
Light	-	+	+	+	+	+	+	+	+	-
% cleavage	9	22	93	91	88	85	78	75	75	7

Figure 48 Salt Challenge EC-I-13, Compound 4. Each of the samples was prepared in the presence of 20 mM sodium phosphate buffer pH 7.0 and 38.5 µM bp pUC19 DNA, and 0-150 mM NaCl in a 20 µL reaction volume. The samples were allowed to preequilibrate at room temperature for 60 min and then were irradiated for 60 min at room temperature in a ventilated Rayonet Photochemical Reactor with eleven 350 nm lamps.
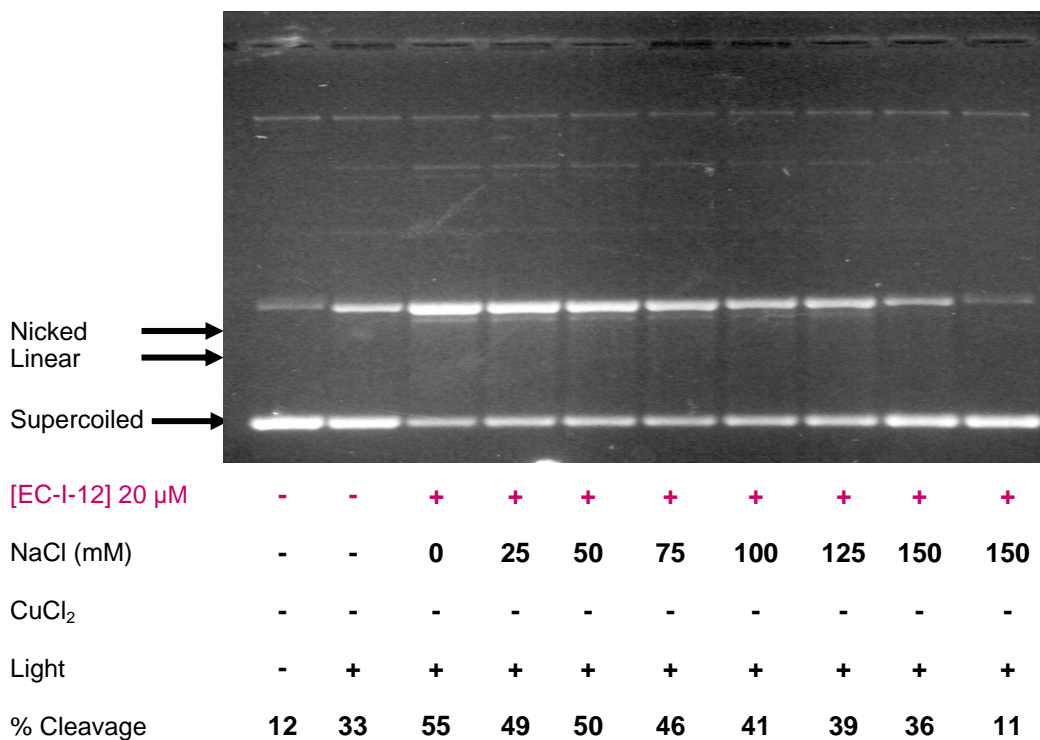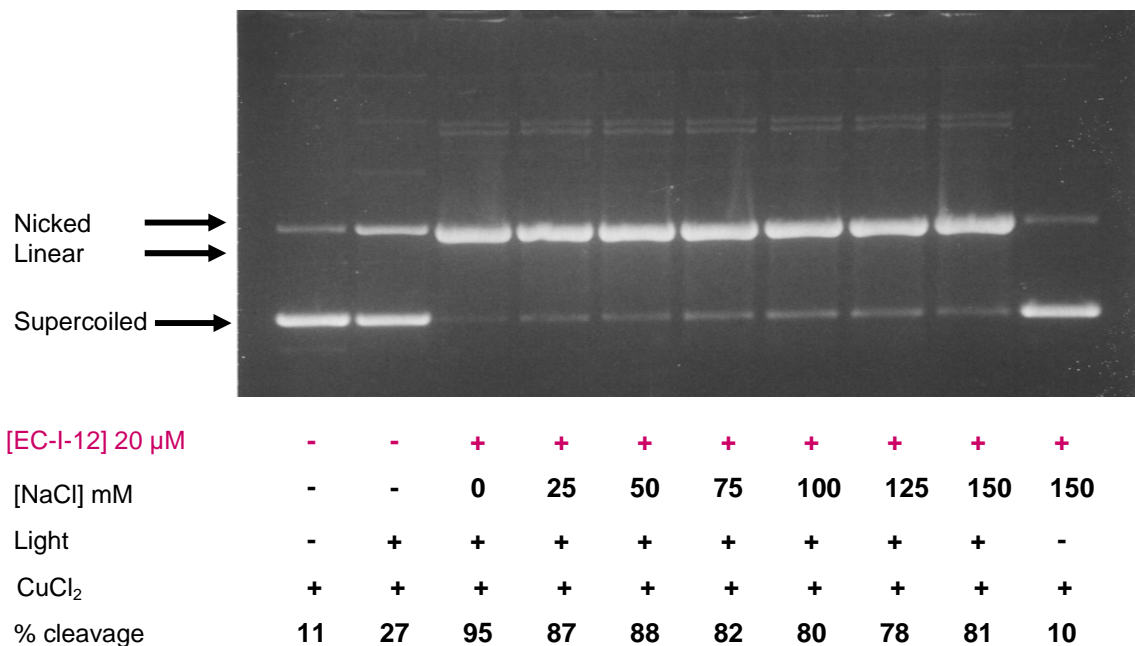

Nicked										
Linear										
Supercoiled										

[AF-I-50] µM	-	-	+	+	+	+	+	+	+	+
[NaCl] mM	-	-	0	25	50	75	100	125	150	150
Light	-	+	+	+	+	+	+	+	+	-
CuCl₂	-	-	-	-	-	-	-	-	-	-
% cleavage	11	10	95	79	72	70	66	63	57	10

Figure 49 Salt Challenge AF-I-50, Compound 5 w/o CuCl₂. Each of the samples was prepared in the presence of 20 mM sodium phosphate buffer pH 7.0 and 38.5 µM bp pUC19 DNA, and 0-150 mM NaCl in a 20 µL reaction volume. The samples were allowed to preequilibrate at room temperature for 60 min and then were irradiated for 60 min at room temperature in a ventilated Rayonet Photochemical Reactor with eight 419 nm lamps.

Nicked										
Linear										
Supercoiled										
[AF-I-50] µM	-	-	+	+	+	+	+	+	+	+
[NaCl] mM	-	-	0	25	50	75	100	125	150	150
CuCl₂	+	+	+	+	+	+	+	+	+	+
Light	-	+	+	+	+	+	+	+	+	-
% cleavage	11	10	95	79	72	70	66	63	57	10

Figure 50 Salt Challenge AF-I-50, w/ CuCl₂. Each of the samples was prepared in the presence of 20 mM sodium phosphate buffer pH 7.0, equimolar copper chloride and 38.5 µM bp pUC19 DNA, 5 µM CuCl₂, and 0-150 mM NaCl in a 20 µL reaction volume. The samples were allowed to preequilibrate at room temperature for 60 min and then were irradiated for 60 min at room temperature in a ventilated Rayonet Photochemical Reactor with eight 419 nm lamps.
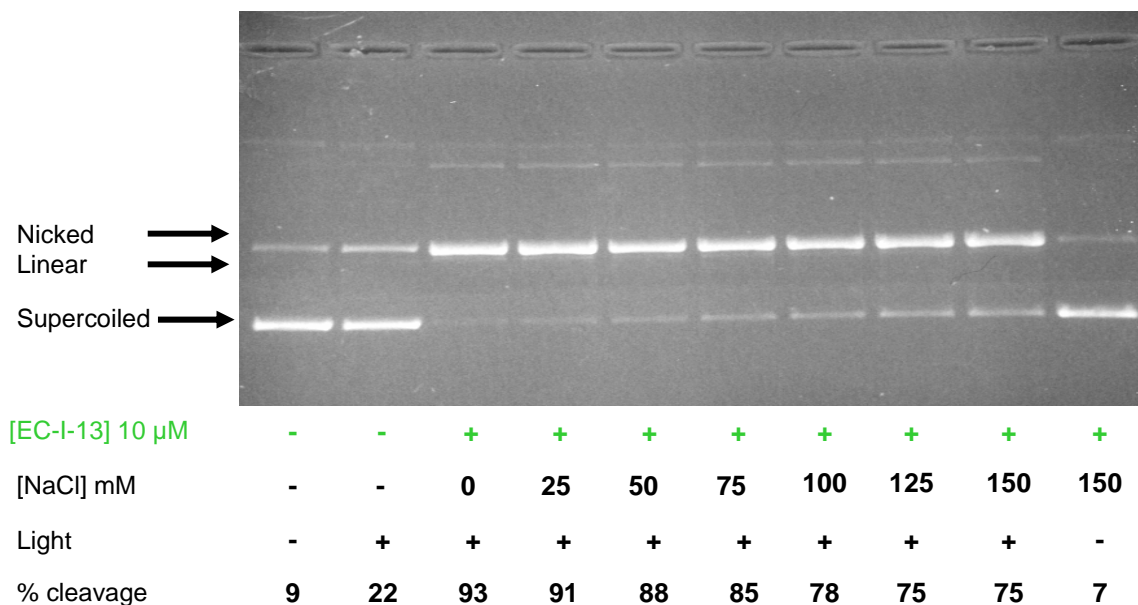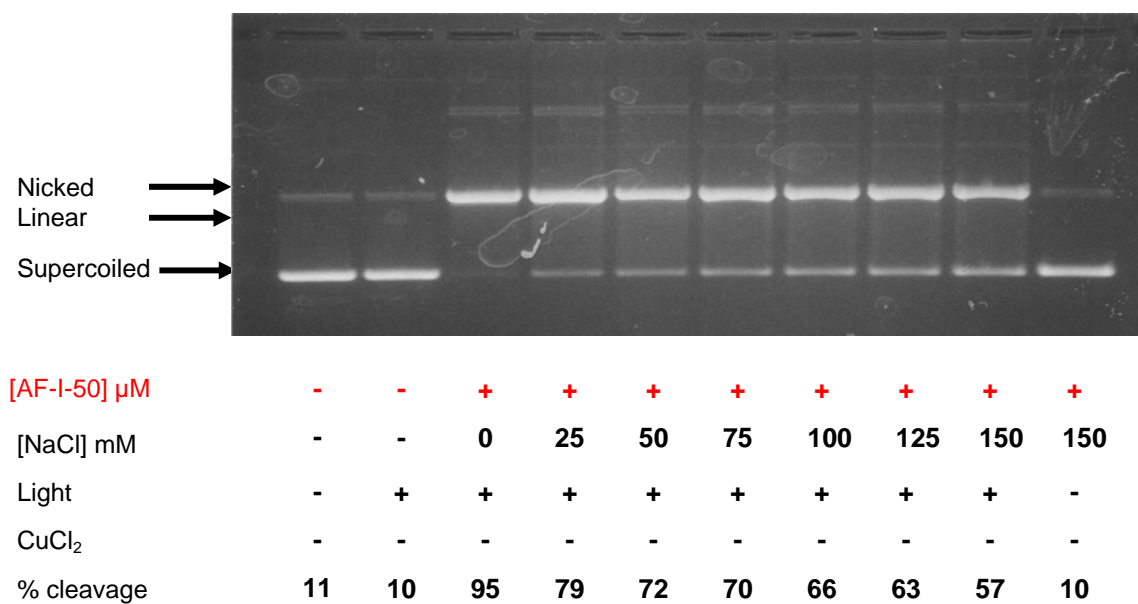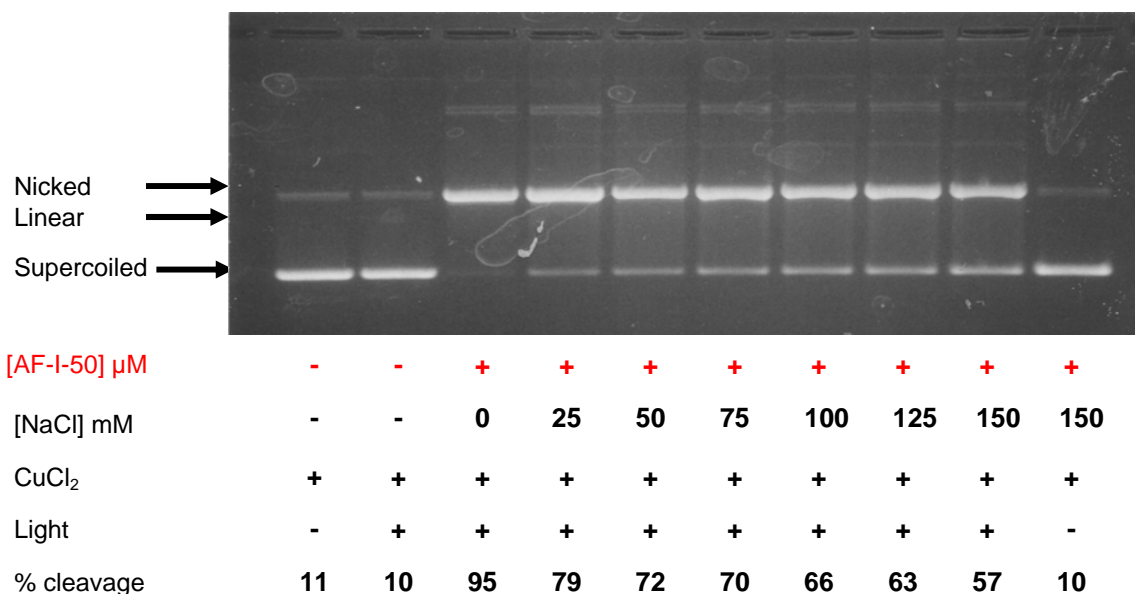

Nicked										
Linear										
Supercoiled										
[MP-I-73] 50 µM	-	-	+	+	+	+	+	+	+	+
[NaCl] mM	-	-	0	25	50	75	100	125	150	150
CuCl₂	-	-	-	-	-	-	-	-	-	-
Light	-	+	+	+	+	+	+	+	+	-
% cleavage	17	25	49	38	33	32	29	28	24	16

Figure 51 Salt Challenge MP-I-73 w/o Cu (II), Compound 6. Each of the samples was prepared in the presence of 20 mM sodium phosphate buffer pH 7.0 and 38.5 µM bp pUC19 DNA, and 0-150 mM NaCl in a 20 µL reaction volume. The samples were allowed to preequilibrate at room temperature for 60 min and then were irradiated at room temperature for 60 min in a ventilated Rayonet Photochemical Reactor with eight 419 nm lamps.

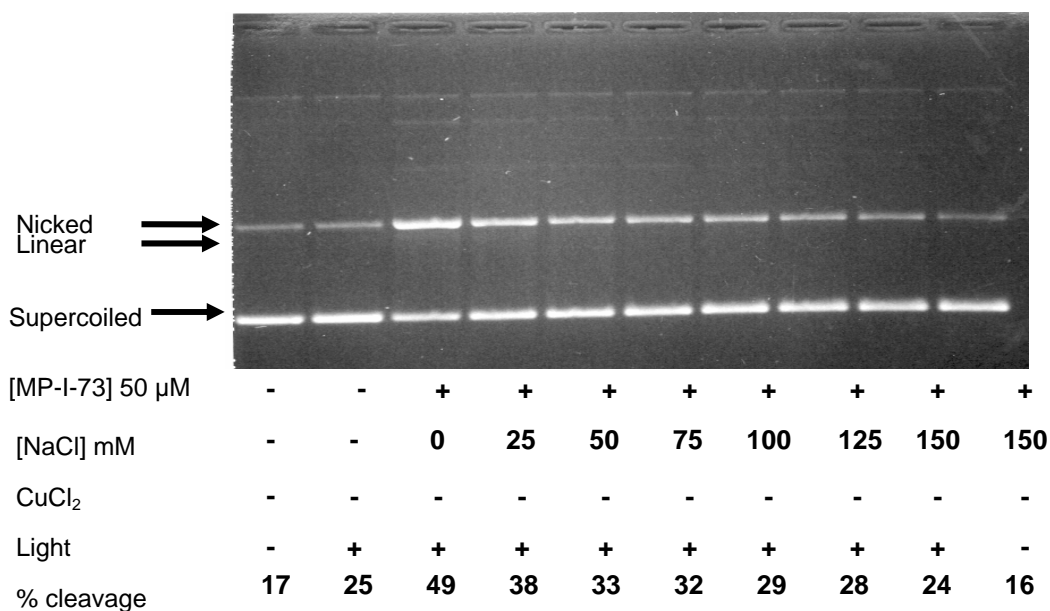|										
[MP-I-73] 50 µM	-	-	+	+	+	+	+	+	+	+
[NaCl] mM	-	-	0	25	50	75	100	125	150	150
CuCl₂	+	+	+	+	+	+	+	+	+	-
Light	-	+	+	+	+	+	+	+	+	-
% cleavage	18	21	91	84	81	77	75	63	67	7

Figure 52 Salt Challenge MP-I-73 w/ Cu (II), Compound 6. Each of the samples was prepared in the presence of 20 mM sodium phosphate buffer pH 7.0, equimolar copper chloride and 38.5 µM bp pUC19 DNA,equimolar copper(II), and 0-150 mM NaCl in a 20 µL reaction volume. The samples were allowed to preequilibrate at room temperature for 60 min and then were irradiated at room temperature for 60 min in a ventilated Rayonet Photochemical Reactor with eight 419 nm lamps.
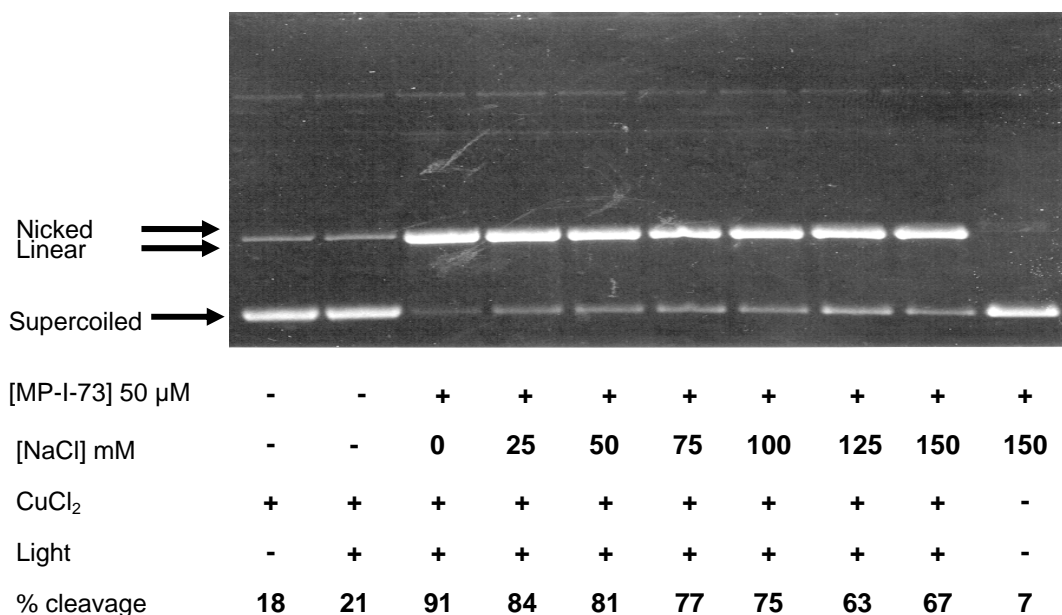
Compound		[Salt]					
		25 mM	**50 mM**	**75 mM**	**100 mM**	**125 mM**	**150 mM**
1		83%	82%	79%	81%	76%	82%
2		16%	40%	41%	49%	49%	58%
3	w/oCu	21%	18%	32%	50%	57%	67%
	w/Cu	13%	12%	21%	25%	28%	23%
4		0%	7%	11%	21%	25%	25%
5	w/oCu	19%	27%	29%	34%	38%	45%
	w/Cu	17%	33%	36%	36%	49%	55%
6	w/oCu	46%	67%	67%	83%	88%	99%
	w/Cu	10%	14%	20%	23%	40%	35%

Table 6 Salt Inhibition Assays, Percent inhibition in the Presence of NaCl. Each of the samples was prepared in the presence of 20 mM sodium phosphate buffer pH 7.0 and 38.5 µM bp pUC19 DNA, and 0-150 mM NaCl in a 20 µL reaction volume. The samples were allowed to preequilibrate at room temperature for 60 min and then were irradiated for 60 min in a ventilated Rayonet Photochemical Reactor under aerobic conditions. Compounds **3**, **5**, and **6** were also tested in the presence of equimolar copper(II).

In the case of compounds **1**, **2**, **3** w/o copper, **5** and **6** w/o copper, moderate to significant reductions in the amount of nicked and linear DNA were observed as the concentration of NaCl was increased. In comparison, compounds **3** and **4** were more robust and remained relatively unaffected when NaCl concentration was increased. In both cases, the % inhibition values were 23% in the presence of 150 mM NaCl.

In this series of experiments, the effect of sodium counter cations on the ability of the investigational compounds to photoconvert supercoiled DNA to nicked or linear forms was examined. In each case, the increasing concentrations of sodium chloride were in the titrated into reaction mixtures. The percent inhibition induced by the competitive sodium cations was calculated using formula **6**. From the values obtained in these experiments, the compounds can be ranked according to their abilities to achieve highest cleavage in the presence of physiological concentrations of sodium chloride (150 mM) as follows: **3** (w/ Cu(II)) > **4** > **6** (w/ Cu (II)) > **5** (w/o Cu (II)) ≈ **5** (w/ Cu (II)) > **2** > **3** (w/o Cu (II)) > **1** > **6** (w/o Cu(II)).

Conclusions

In this thesis, we describe several phenazine and acridine-based intercalators that are able to effectively mediate photocleavage of pUC19 plasmid DNA through a combination of type one and/or type two photocleavage pathways. Compound **5** proved to be the most effective DNA photocleaver, followed by **2**, **4**, **3**, **6** and finally **1**, when thermal stability and ability to cleave at physiological concentrations of NaCl is taken into account. T_m data have been presented, suggesting strong binding of compounds **2**, **4**, and **5** to double-helical DNA. (In the T_m measurements the compounds were ordered based upon their ability to bind CT-DNA as follows, **2** > **5 w/Cu(II)** > **1** ≈ **5 w/o Cu(II)** > **4** > **3** > **6 w/Cu(II)** > **6 w/o Cu(II)**). In general, photocleavage activity was found to show a strong correlation to ΔT_m values. The viologen linker employed in the reference compound **2** was found to induce superior binding and photocleavage compared to the more flexible linker employed in its analogue compound **1**. Additionally, the smaller more constrained pyridine linker employed in compound **5** was determined to be superior to the longer pyridine linker employed in the analogous compound **6** in terms of overall photocleavage efficiency. In an attempt to evaluate how photo-induced damage and DNA-binding might be affected by competitive ions, a series of salt inhibition experiments was conducted. We have demonstrated that compounds **3** w/Cu and **4** show the most robust photocleavage when challenged with physiological concentrations of sodium chloride. Several of the compounds were designed to bind copper. Thus, copper was found to induce significant enhancement in DNA photocleavage by all three putative copper binding compounds (**3**, **5** and **6**). It is notable that the metal binding planar compound **3** was the most resistant to inhibition induced by competitive sodium cations.

Among the four new compounds investigated in this thesis (**1**, **3**, **4**, and **5**), I have found that the linked bis-acridine derivative **5** (AF-I-50) possesses the highest potential for use in PDT. This determination was based upon the ability of this compound to effectively induce ≥ 90 % photocleavage in pUC19 DNA at concentrations as low as 5 μM. Compound **5** demonstrated significant DNA binding as indicated by pronounced bathochromicity and hypochromicity, its large ΔT_m value as well as by the changes in DNA mobility noted in gel shift assays. In addition, compound **5** induced photoconversion of DNA at high levels when challenged with sodium chloride. Compound **5** demonstrated good results the binding studies, and also exhibited robust performance through the entire series of experiments, and is therefore considered to be the most promising of the new compounds. This helps support the idea of structure-based drug design as an effective method to develop new and more effective DNA-photocleavage agents.

References

1.   Ackroyd, R., Kelty, C., Brown, N., and Reed, M., *The history of photodetection and photodynamic therapy.* Photochemistry and Photobiology, 2001. **74**: p. 656-669.

2.   Daniell, M.D. and Hill, J.S., *A history of photodynamic therapy.* Australian and New Zealand Journal of Surgery, 1991. **61**: p. 340–348.

3.   Spikes, J.D., in *Primary Processes in Biology and Medicine*. 1985, Plenum Press: New York. p. 209-227.

4.   Raab, O., *Uber die Wirkung fluorezierender Stoffe auf Infusorien.* Zeitung Biology, 1900. **39**: p. 524-526.

5.   Prime, J., *Les accidents toxiques par l'eosinate de sodium*. 1900, Paris: Jouve and Boyer.

6.   von Tappeiner, H., and Jesionek, A., *Therapeutische versuche mit fluoreszierenden stoffen.* Muench Medicine Wochenschr, 1903. **47**: p. 2042-2044.

7.   vonTappeiner, H. and Jodlbauer, A., *Die sensibilisierende Wirkung fluorezierender Substanzer Gesammte Untersuchungen uber die photodynamishe Erscheinerung*. 1907, Leipzig: F.C. Voger.

8.   Finsen, N.R., *Phototherapy*. 1901, London: Edward Arnold.

9.   Hausman, W., *Die sensiblisierende wirkund des hematoporphyrins.* Biochemistry Journal, 1911. **30**: p. 276-316.

10.   Meyer-Betz, F., *Untersuchungen uber die biologische photodynamische Wirkung des Hematoporphyrins und anderer Derivative des Blu und Galenafarbstoffs.* Deutsch Arch. Klin, 1913. **112**: p. 476-503.

11.   Auler, H., and Banzer, G., *Untersuchungen über die Rolle der Porphyrine bei Geschwulstkranken Menschen und Tieren.* Z Krebsforsh, 1942. **53**: p. 65-68.

12.   Cremer, R., Perryman, P., and Richards, D., *Influence of light on the hyperbilirubinaemia of infants.* Lancet, 1958. **1**: p. 1094-1097.

13.   Schwartz, S.K., Abolon, K., and Vermund, H., *Some Relationships of porphyrins, X-rays and tumors.* University of Minnesotta Medical Bulletin, 1955. **27**: p. 7-8.

14.   Lipson, R.L., Baldes, E.J., and Olsen, A.M., *The use of a derivative of hematoporphyrin in tumor detection*. Journal of the National Cancer Institute, 1961. **26**: p. 1-11.

15   Dougherty, T.J., Grindey, G.B., Fiel, R., Weishaupt, K.R., and Boyle, D.G., *Photoradiation therapy II. Cure of animal tumors with hematoporphyrin and light.* Journal of the National Cancer Institute, 1975. **55**: p. 115-121.

16   Dougherty, T.J., *Photoradiatioin therapy for the treatment of malignant tumors.* Cancer Research, 1978. **38**: p. 2628-2635.

17   Dougherty, T.J., *Photoradiation in the treatment of recurrent breast carcinoma.* Journal of the National Cancer Institute, 1979. **62**: p. 231-237.

18.   Lam S., Muller N.L., Miller R.R., Kostashuk, E.C., Szasz, I.J., Leriche, J.C., Lee-Chuy, E. *Predicting the response of obstructive endobronchial tumors to photodynamic therapy*. Cancer, 1986. **58**: p. 2298.

19.   Kelly, J.F., Snell, M.E., and Berenbaum, M.C., *Photodynamic destruction of human bladder carcinoma.* British Journal of Cancer, 1975. **31**: p. 237-244.

20. Dougherty, T.J., *Photoradiation in the treatment of recurrent breast carcinoma.* Journal of the National Cancer Institute, 1979. **62**: p. 231-237.

21. Diamond, I., *Photodynamic therapy of malignant tumours.* Lancet, 1972. **2**: p. 1175-1177.

22. Krasheninnikoff, M., Ellitsgaard, N., and Rogvi-Hansen, B., *No effect of low power laser in lateral epicondylitis.* Scandinavian Journal Rheumatology, 1994. **23**(5): p. 260-263.

23. Wertz, R.L., *Caution- Therapeutic Lasers in Use...Don't Get Burned! : A Therapeutic Laser Buyer's Guide*, in *Avicenna Class IV Laser Therapy*. 2004.

24. Sharman, W.M., Allen, C.M., and van Lier, J.E., *Photodynamic therapeutics: basic principles and clinical applications*. Therapeutic Focus.1999. **4**: pp. 507-517.

25. Detty, M.R., Gibson, S.L., and Wagner, S.J., *Current Clinical and Preclinical Photosensitizers for Use in Photodynamic Therapy.* Journal of Medicinal Chemistry, 2004. 47(16): p. 3897-3911.

26. Castano, A.P., Demidova, T.N., and Hamblin, M.R, *Mechanisms in photodynamic therapy: part one-photosensitizers, photochemistry and cellular localization.* Photodiagnosis and Photodynamic Therapy, 2004. **1**: p. 274-293.

27. Dennis, E.J., *Photodynamic therapy for cancer.* Nature Reviews: Cancer, 2003. **3**: p. 380-387.

28. Ben-Hur, E. and Rosenthal, I., *The phthalocyanines: synthetic porphyrin-like dyes with an improved potential for cancer phototherapy. Photosensitization of Chinese hamster cells by chloroaluminum phthalocyanine.* Photochemistry and Photobiology, 1985. **42**: p. 129-133.

29. Bodor, N. S., Karsa, D. R., and Stephenson, R. A., *Chemical Aspects of Drug Delivery Systems;* Royal Society of Chemistry: London, 1996.

30. Eisenberg, A. *Polycaprolactone-b-poly(ethylene Oxide) Block Copolymer Micelles as a Novel Drug Delivery Vehicle for Neurotrophic Agents FK506 and L-685,818.* Bioconjugate Chemistry, 1998. **9**: p. 564.

31. Han, J. H., Krochta, J.M., Kurth, M.J., and Hsieh, Y.L., *Lactitol-Based Poly(ether polyol) Hydrogels for Controlled Release Chemical and Drug Delivery Systems.* Journal of Agriculture Food Chemistry 2000, 48, 5278.

32. Langer, R., Chiba, M., and Hanes, J., *Synthesis and Characterization of Degradable Anhydride-co-imide Terpolymers Containing Trimellitylimido-L-tyrosine: Novel Polymers for Drug Delivery.* Macromolecules,1996. **29**: p. 5279.

33. Konan, Y.N., Gurny, R., and Allemann, E., *Invited Review State of the art in the delivery of photosensitizers for photodynamic therapy.* Journal of Photochemistry and Photobiology B: Biology, 2001. **66**: p. 89-106.

34. Lu, K.K. and Ogilby, P.R., *A time-resolved study of singlet molecular oxygen formation in a solution phase photosensitized reaction: a new experimental technique to examine the dynamic of quenching by oxygen.* Journal of Physical Chemistry, 1987. **91**: p. 1611-1617.

35. Barton, J.K. and Raphael, A.L., *Photocleavage of nucleic acids.* Chemical Reviews, 1998. **98**: p. 1171-1200.

36. Cadet, J. and Vigny, P., *The Photochemistry of Nucleic Acids*, in *Bioorganic Photochemistry*, H. Morrison, Editor. 1990, Wiley: New York. p. 1-272.

37.   Dunn, D.A., Kochevar, I.E. *Photosensitized Reactions of DNA: Cleavage and Addition*, in *Bioorganic Photochemistry*, H. Morrison, Editor. 1990, Wiley: New York. p. 273-315.

38.   Dysart, J.S. and Patterson, M.S., *Characterization of Photofrin photobleaching for singlet oxygen dose estimation during photodynamic therapy of MLL cells in vitro.* Physics in Medicine and Biology, 2005. **50**(11): p. 2597.

39.   Fingar, V.H., Wieman, T.J., and Haydon, P.S., *The effects of thrombocytopenia on vessel stasis and macromolecular leakage after photodynamic therapy using Photofrin.* Photochemistry and Photobiology, 1997. **66**: p. 513-517.

40.   Inaba, K., Turley, S., Yamaide, F., Iyoda, T., Mahnke, K., Inaba, M., Pack, M., Subklewe, M., Sauter, B., Sheff, D., Albert, M., Bhardwaj, N., Mellman, I., and Steinman R., *Efficient presentation of phagocytosed cellular fragments on the major histocompatibiolity complex class II products of dendritic cells.* Journal of Experimental Medicine, 1998. **188**: p. 2163-2173.

41.   Kohs, J.S. and Levine, J.S., *Apoptosis and autoimmunity.* Current Opinions Nephrology Hypertension, 1997. **6**: p. 259-266.

42.   Star, W.M., *Destruction of rat mammary tumor and normal tissue microcirculation by hematoporphyrin derivative photoradiation observed in vivo in sandwich observation chambers.* Cancer Research, 1986. **46**: p. 2532-2540.

43.   Fingar, V.H., *Analysis of acute vascular damage after photodynamic therapy using benzoporphyrin derivative (BPD).* British Journal of Cancer, 1999. **79**: p. 1702-1708.

44.   Dolmans, D.E.J.G.J., Kadambi, A., Hill, J.S., Waters, C.A., Robinson, B.C., Walker, J.P., Fukumura D. and Jain, R.K., *Vascular Accumulation of a Novel Photosensitizer, MV6401, Causes Selective Thrombosis in Tumor Vessels after Photodynamic Therapy.* Cancer Research, 2002. **62**(7): p. 2151-2156.

45.   Busch, T.M., Wileyto, E.P., Emanuele, M.J., Del Piero F., Marconato, L., Glatstein, E., and Koch, C.J., *Photodynamic Therapy Creates Fluence Rate-dependent Gradients in the Intratumoral Spatial Distribution of Oxygen.* Cancer Research, 2002. **62**(24): p. 7273-7279.

46.   Chen, Q., Chen, H., and Hetzel, F.W., *Tumor oxygenation changes post-photodyamic therapy.* Photochemistry and Photobiology, 1996. **63**: p. 128-131.

47.   Fingar, V.H. and Henderson, B.W., *Relationship of tumor hypoxia and response to photodynamic therapy.* Cancer Research, 1987. **47**: p. 3110-3114.

48.   Dolmans, D.E.J.G.J., Fukumura, D., and Jain, R.K., *Photodynamic therapy for cancer.* Nature Reviews: Cancer, 2003. **3**: p. 380-387.

49.   Spector, W.S., *Handbook of Biological Data*; W.B. Saunders Company: Philadelphia, PA, 1956, p.52.

50.   Bryan, S.E., Vizard, D.L., Beary, D.A., LaBiche, R.A., and Hardy, K.J., *Partitioning of zinc and copper within subnuclear nucleoprotein particles.* Nucleic Acids Research, 1981. **9**: p. 5811-5823.

51.   Maniatis, T., Sambrook, J., Fritsch, E.F. <u>Molecular Cloning A Laboratory Manual</u>. 1989. Cold Springs Harbor: Cold Springs Harbor Laboratory Press.

52.   Fernández, M.J., Grant, K.B., Herraiz, F., Yang, X., and Lorente, A., *DNA photocleavageby dicationic bisintercalants.* Tetrahedron Letters, 2001. **42**: p. 5701-5704.

53.   Fernández, M.-J., Wilson, B., Palacios, M., Grant, K.B., and Lorente, A. *Copper-Activated DNA Photocleavage by a Pyridine-Linked Bis-Acridine Intercalator*. Bioconjugate Chemistry, accepted 2006.